Thesis for the degree of Doctor of Philosophy

Multicarrier communication systems with low sensitivity to nonlinear amplification

Marc Deumal Herraiz

Enginyeria i Arquitectura La Salle
Universitat Ramon Llull

Barcelona 2008

Multicarrier communication systems with low sensitivity to nonlinear amplification

Marc Deumal Herraiz
Research Group in Electromagnetism and Communications (GRECO)
Enginyeria i Arquitectura La Salle
Universitat Ramon Llull
Quatre Camins, 2
08022 Barcelona, Spain
E-mail: mdeumal@salle.url.edu

Advisor: Dr. Joan Lluís Pijoan Vidal
Enginyeria i Arquitectura La Salle, Universitat Ramon Llull, Barcelona, Spain.

This thesis has been prepared using LaTeX.

A la Carme i als meus pares

Abstract

We are now facing a new information age with high demand of wireless communication systems. New services such as data and video require achieving reliable high-speed transmissions even in high mobility scenarios. Moreover, the difficulty to allocate so many wireless communication systems in the limited frequency band in addition to the demand for long battery life requires designing spectrum and power efficient transceivers. Multicarrier communications based on orthogonal frequency division multiplexing (OFDM) have grown in popularity due to its ability to fulfill most of the requirements of such systems. However, among other challenges, reducing the sensitivity to nonlinear amplification has become a design key. When a nonlinear device is present at the transmitter, both a spectral spreading and an increase of the error probability occur. There are many strategies to reduce this performance degradation such as linearization, post-processing and reducing the envelope fluctuations of the transmitted signal. OFDM suffers from large envelope fluctuations that increase its sensitivity to nonlinear amplification, therefore, reducing the envelope fluctuations in such systems becomes a key issue.

In this thesis the sensitivity of OFDM-based multicarrier systems to nonlinear amplification is analyzed and efficient ways to overcome this problem are considered. The focus is mainly on the problem of reducing the envelope fluctuations. Therefore, a study of the signal envelope metrics, namely peak-to-average power ratio (PAPR) and cubic metric (CM), is also presented. From the presented analysis, several new techniques for OFDM and multicarrier spread-spectrum systems (MC-SS) systems and faster low-complexity suboptimal methods capable of approaching the optimal solution with high accuracy are proposed. For MC-SS, the design of a post-processing technique in the form of a multiuser detector for nonlinearly distorted MC-SS symbols is also addressed.

Keywords: orthogonal frequency division multiplexing (OFDM), multicarrier spread-spectrum (MC-SS), single-carrier FDMA (SC-FDMA), nonlinearity, peak-to-average power ratio (PAPR), cubic metric (CM), multiuser detection (MUD).

Acknowledgments

My PhD is almost over but I can not finish it without looking back and thanking all the people that in one way or the other helped me to make it possible. It is not difficult to imagine that I would like to start by giving my deepest special thanks to *my* Carme. For her infinite support, for being always there no matter how far I am and how long it takes me to come back, but specially for sharing all my dreams. Special thanks to my parents who always trusted me and encouraged me to go on. You know there are no words to thank you all you have done for me during the last 28 years.

To my advisor Joan Lluís Pijoan, for believing in me and for pushing me to go further and further. Thanks also for giving me always the freedom to draw new paths in our research activities. I am also very grateful to the head of our department, David Badia, who has always been so patient, honest and considerate. I would like to give my extreme thanks to my *unofficial* co-advisor, but undoubtedly very good friend, Ali Behravan. I consider myself very lucky for having had the chance to cooperate with him and, of course, for all the fun we had in Göteborg and Stockholm. Thanks also for proof-reading this thesis so accurately.

I would like to give my special thanks to Arne Svensson for his excellent hospitality during the six months I spent at Chalmers University of Technology. Thanks also for arranging everything so that I could feel myself to be another one in the Communication Systems Group. My best thanks also to Göran Klang for accepting me as a guest researcher at Ericsson and for taking care of every detail around it. I hope that our future cooperation is as worth for Ericsson as it will be for me. I would also like to thank Mehmet Safak who as the chairman of COST–289 has always been very enthusiastic with my research activities and with my cooperation with other institutions within the COST–289 framework. I am also very thankful to Dušan Kocur and Pavol Galajda for our joint cooperation and for inviting me at the Technical University of Košice.

During my PhD I had the opportunity to meet many senior researchers that were always open for discussion and to spread their wide knowledge in the communications field. First of all, I would like to thank Carles Vilella, from my university in Barcelona, for introducing me in the research world some years ago and for giving me always many advices to continue progressing. I am specially grateful to Thomas Eriksson with whom I had the chance to share and discuss my ideas during my research stay at Chalmers, where it all began. I am also specially grateful to Robert Baldemair, my

always available mentor during the research stay at Ericsson, who among many other things showed me how to move from academy to industry type of research. Thanks also to Miquel Ribó, David Miralles and Joan Claudi Socoró in my university for all the nice moments and all the worth discussions. And, thanks also to Erik Ström and Tony Ottosson at Chalmers for sharing their outstanding knowledge in digital communications. Finally, I would like to give my best thanks to Sorour Falahati for proof-reading part of this thesis.

To all my colleagues from the Department of Communications and Signal Theory, La Salle and Ramon Llull University: Joan Ramon, Antonio, Simó, Pajares, Albert, Pablo, Sevillano, Xuti, Rosa, Vilasís, Carles Garriga, Pep Martorell, etc. But specially, to my roommates Ricard Aquilué, Pau Bergadà and Ismael Gutiérrez (sorted alphabetically) with whom I had so many discussions and shared such a great time. And of course, my best thanks to all the people I have been involved with during these years either at Chalmers University of Technology, Ericsson Research or at the Technical University of Košice.

My deepest thanks to my new family in Stockholm: Ali, Sorour and Jon. This time together was something big but I am sure it was just the beginning of something huge. We still have to spend much more time playing innebandy, guitar, climbing, partying, traveling, etc. See you at the wedding! Thanks also to my precious new friends Reihnaeh, Shahroh, their baby, Stefano, etc. for doing all your best so that I have a great time in Stockholm. And at last but not at least to all my friends with whom I shared such a long time climbing, biking, skiing or just messing around. Grau, Miriam, Alan, Laura, Che, Marta, etc. at my birth town. Mace, Marisa, Pino, Laura, Ernest, Tere, Joan, Montse and Mario for welcoming Carme and me to our new town.

Marc Deumal Herraiz
Stockholm, May 2008

This thesis received the first Rosina Ribalta award from Epson Foundation to the best project of doctoral thesis in the field of information and communication technologies in 2008.

The work presented in this thesis has been funded by the FPI Scholarship from the Ministry of Education and Science in the Spanish Government and the European action COST289 "Spectrum and Power Efficient Broadband Communications".

About the author

Marc Deumal Herraiz received his BSc and MSc degrees in Telecommunications in 2001 and 2003, respectively, from Enginyeria i Arquitectura La Salle, Universitat Ramon Llull (URL), in Barcelona. Since 2004 he is a FPI PhD Fellow from the Spanish Government at the Research Group in Electromagnetism and Communications (GRECO) in La Salle, URL.

Between 2004 and 2007 he was involved with the European action COST289 "Spectrum and Power Efficient Broadband Communications". In 2004/05 he spent six months as a guest researcher at Chalmers University of Technology, Sweden, cooperating within the framework of COST289 and in 2008 he spent five months at Ericsson Research in Stockholm where he worked on the uplink of Long Term Evolution (LTE). He is reviewer of several journals including *Springer Journal on Wireless Personal Communications*, *EURASIP Journal on Wireless Communications and Networking*, and *IEEE Communication Letters*. In 2008 he received the first Rosina Ribalta award from Epson Foundation to the best project of doctoral thesis in the field of information and communication technologies. His research interests are in digital signal processing, communications, software defined radio and vehicular technology.

Research projects

As a member of GRECO, La Salle, URL, he participated in several research projects related to the digital communications field.

From September 2001 to June 2003 he worked on the design of a software defined radio based digital platform, named as SODIO. The digital platform consists mainly of FPGA devices, high-speed high-resolution A/D/A converters, communication specific ASICs and several input-output buses that assure sufficient connectivity with other platforms and devices. This work was done during the Master degree studies and was presented as the Master's thesis. The funding was provided by La Salle under the internal projects PGR-PR2001-01 "Research on Software Radio Techniques" and PGR-PR2003-06 "Advanced Receivers with Software Radio (ARSODIO)".

Between 2003 and September 2004 he participated in the internal project from La Salle PGR-PR-2004-06 "Study of software architectures. Fitting to SODIO platform",

where software interfaces with SODIO devices and input-output buses were implemented.

On September 2004 he joined the so-called *Antarctic project*: REN2003-08376-C02-01 "Characterization and modeling of the Antarctic ionospheric channel: Advanced HF communications" funded by the Ministry of Education and Science from the Spanish Government. The aim of the Antarctic project is to design of a robust unidirectional system for long haul HF communications through the ionosphere. The radimodem must be capable of transmitting data with high reliability from a geomagnetic sensor located at the Spanish Antarctic Base in Livingston Island to the Ebro Observatory in Spain. Moreover, due to power supply restrictions in the Spanish Antarctic Base low power transmissions are required.

Within the Antarctic project the author has mainly participated on the design of the hardware and software for the transmitter and receiver (which are based on the SODIO digital platform) and on the design of the preliminary systems for data transmissions. Two major advanced modulation techniques are being evaluated: direct-sequence spread-spectrum (DS-SS) signaling and orthogonal frequency division multiplexing (OFDM).

DS-SS signaling consists in mapping m data bits into one of the $M = 2^m$ spreading codes. At the receiver, the transmitted bits are obtained by correlating the received time-frequency synchronized signal with the M spreading codes. Maximum correlation value determines the most probable transmitted spreading code, i.e. the most probable transmitted group of m bits. The advantages of this technique are, first, that the spectral efficiency can be increased by hardly decreasing the signal-to-noise ratio (SNR) and, second, that accurate channel estimation is not required. The downside is that the computational complexity grows exponentially with m. In an OFDM system the data are transmitted over a number of parallel frequency channels, each being modulated by a baseband PSK or QAM symbol. The advantages of this technique are that no complex equalization is required, high spectral efficiency can be achieved and it has an intrinsic robustness against narrow-band interference. The downside are its sensitivity to nonlinear amplification and the sensitivity to the frequency offset.

In general, power amplifiers introduce some distortion to the transmitted signal which reduce the performance of the communication systems. OFDM signals are known to be much more sensitive to nonlinear amplification than single carrier systems. Therefore, special attention has to be paid on the physical layers of the OFDM systems in order to reduce their performance degradation as much as possible. An easy and effective way to achieve it is by setting the working point of the amplifier far enough from saturation so that the signal is always linearly amplified. However, since OFDM suffers from large envelope fluctuations such a solution is impractical as it requires an extremely inefficient use of the high power ampligier (HPA). This thesis analyzes the sensitivity of OFDM to nonlinear amplification and addresses the design of efficient

ways to reduce it so that OFDM becomes a good candidate for the implementation of the radiomodem.

Cooperation with other institutions

During the four years of the PhD the author cooperated with different universities and research centers. From 2004 to 2007, he participated in the European action COST289 "Spectrum and Power Efficient Broadband Communications" which gave him the chance to discuss the ideas with other researchers from many different institutions. Within the COST289 framework the author wants to specially highlight the Chalmers University of Technology from Göteborg, Sweden, since most of the contributions presented in this thesis are the result of the cooperation with this institution. Moreover, he also wants to mention the Technical University of Košice, Slovakia, for the joint contribution in multiuser detection.

During the first halve of 2008 the author was involved with Ericsson Research in Stockholm working on the physical layer of the future generation of wireless systems. The most recent contributions presented in this thesis were undertaken in this company.

Summary of contributions

This thesis is the result of the work carried out in the following contributions:

- M. Deumal and A. Behravan,"Unified analysis of nonlinear amplification effects and signal metrics in OFDM systems", *IEEE Transactions on Wireless Communications*, submitted for publication, June 2008.
- M. Deumal and A. Behravan,"Analysis of nonlinear amplification effects and signal metrics in OFDM systems", Ericsson Research, Limited Internal Report, June, 2008.
- M. Deumal and Robert Baldemair,"Signal metrics and nonlinearity effects in LTE uplink", *Proceedings of IEEE Global Communications Conference*, submitted for publication, March, 2008.
- M. Deumal, "Signal metrics and nonlinearity effects in LTE uplink", Ericsson Research, Limited Internal Report, March, 2008.
- M. Deumal, A. Behravan and J.L. Pijoan,"On cubic metric reduction in OFDM systems by tone reservation", *IEEE Transactions on Communications*, submitted on November 2007, under revision for publication since March 2008.
- M. Deumal, A. Behravan, T. Eriksson and J.L. Pijoan,"Evaluation of performance improvement capabilities of PAPR-reducing methods", *Springer Journal on Wireless Personal Communications*, October 2007.

- J. Krajňák, M. Deumal, P. Pavelka, D. Kocur, J.L. Pijoan and P. Galajda,"Multiuser detection of nonlinearly distorted MC-CDMA symbols by microstatistic filtering", *Springer Journal on Wireless Personal Communications*, October 2007.

- M. Deumal, A. Behravan, T. Eriksson and J.L. Pijoan,"Constrained clipping for Peak Power reduction of multicarrier systems by Tone Reservation", in *Proceedings of IEEE Vehicular Technology Conference Spring*, pp. 2195 - 2199, April 2007.

- M. Deumal, J.L. Pijoan, I. Gutiérrez and A. Behravan, "Peak reduction of multicarrier systems by Controlled Spectral Outgrowth", in *Proceedings of IEEE International Conference on Acoustics, Speech and Signal Processing*, vol. 4, pp. 317 - 320, May 2006.

- M. Deumal, I. Gutiérrez and J.L. Pijoan, "PAPR reduction in orthogonal MC and MC-SS systems", *2nd COST289 Workshop: Special topics on 4G systems, COST 289: Spectrum and Power Efficient Broadband Communications*, Antalya, Turkey, July 2005.

- M. Deumal, C. Vilella, J.L. Pijoan and P. Bergadà, "Partially Clipping Method for the Peak-to-Average Power Ratio (PAPR) reduction in OFDM", in *Proceedings of IEEE International Symposium on Personal, Indoor and Mobile Radio Communications*, vol. 1, pp. 464 - 468, September 2004.

As it was previously stated this thesis is related to the project REN2003-08376-C02-01 "Characterization and modeling of the Antarctic ionospheric channel: Advanced HF communications" whose final goal is to implement a radiomodem capable of transmitting data from a geomagnetic sensor in the Spanish Antarctic Base to the Ebro Observatory. The work of the author within this project is mainly to participate on the design of the required equipments and on the design of the preliminary systems for data transmissions. The design and implementation of the equipments has been presented in different conferences. The most important contributions in which he was involved are:

- C. Vilella, P. Bergadà, M. Deumal, J.L. Pijoan and R. Aquilué, "Transceiver Architecture and Digital Down Converter Design for a Long Distance, Low Power HF Ionospheric Link", in *Proceedings of IET Ionospheric Radio Systems and Techniques*, pp. 95 - 99, July 2006.

- C. Vilella, D. Badia, J.L. Pijoan, M. Deumal, M. Ribó, J.R.Regué, "On site receiver testing. Application to long distance HF links", in *International Symposium on Electromagnetic Compatibility, EMC Europe*, September 2006, Barcelona.

- P. Bergadà, C. Vilella, M. Deumal and J.L. Pijoan, "SODIO: A Software Radio Platform for advanced HF communications", *1st COST289 Workshop, COST 289: Spectrum and Power Efficient Broadband Communications*, Budapest, Hungary, July 2004.

- M. Deumal and C. Vilella and J. L. Pijoan, "Software Radio Platform", in *Proceedings of Simposium Nacional de la Unión Científica Internacional de Radio, URSI*, September 2003, in Spanish.

Regarding the design of the preliminary system for data transmission two major modulation techniques are being evaluated: Direct-Sequence Spread-Spectrum Signaling and Orthogonal Frequency Division Multiplexing. The most important contributions in which he was involved are:

- R. Aquilué, P. Bergadà, M. Deumal and J.L. Pijoan, "Multicarrier symbol design for HF transmissions from Antarctica based on real channel measurements", in *Proceedings of IEEE Military Communications Conference*, pp. 1-7, October 2006.

- M. Deumal, C. Vilella, J.C. Socoró, R.M. Alsina and J.L. Pijoan, "A DS-SS Signaling Based System Proposal for Low SNR HF Digital Communications", in *Proceedings of IET Ionospheric Radio Systems and Techniques*, pp. 128 - 132, July 2006.

Contents

Part II: Extended analysis and solutions

Part I

Overview

Chapter 1

Introduction

Today's demands for wireless communication systems include reliability, high-speed data transmission, high mobility and spectrum and power efficiency. Orthogonal frequency division multiplexing (OFDM) based multicarrier communications have recently gained in popularity due to their ability to fulfill most of the requirements of such systems. However, its sensitivity to both frequency offset and nonlinear amplification degrades its performance severely, thus, representing the major drawback of such transmission schemes. If a frequency offset occurs at the input of the OFDM demodulator, the error probability increases drastically due to the overlapping power spectra between neighboring subcarriers. On the other hand, since the time-domain signal envelope suffers from large fluctuations, a large distortion is introduced when it is fed to a nonlinear device. Most of the components in the analog stages of the transmitter and receiver sides do not show a perfectly linear behavior, nevertheless the major source of nonlinearity (NL) and, hence, the major source of distortion, is basically caused by the transmitter high power amplifier (HPA), specially if high power efficiency and low cost transceivers are desired. One should take into account that signals with large envelope fluctuations require power amplifiers with a large linear region operating far from the saturation point. In other words, such transmission schemes require expensive power amplifiers and high power consumption. Reducing the sensitivity to nonlinear amplification is of special relevance for mobile terminals, i.e. in the uplink direction, due to the importance of the low power consumption and cost. For the base station, i.e. in the downlink direction, using low cost and low power consuming HPA, although far from irrelevant, is not such an important design key.

When an OFDM signal undergoes nonlinear distortion spectral spreading and an increase in the error probability occurs. Both are mainly caused by the distortion term introduced by the nonlinearity. However, for low number of subcarriers the non-constant attenuation and rotation of the constellation introduced by the nonlinearity plus the fact that the distortion term is not Gaussian distributed, increase the error probability even further. For large number of subcarriers a constant attenuation and rotation of the constellation occurs. However, this is compensated at the receiver by the channel equalization block and, therefore, it has no effect on the error probability.

In multicarrier spread-spectrum (MC-SS) systems not only the number of subcarriers affects the performance of the system but also the type of spreading code, the number of active codes, the spreading factor and the technique used to combine both multicarrier communication and spread-spectrum.

In order to predict the degradation introduced by a nonlinearity without having to perform an extensive study, it is customary to compute the envelope fluctuations of the transmitted signal. The larger the envelope fluctuations are the larger the degradation is expected. The most common signal metrics are the so-called peak-to-average power ratio (PAPR) and cubic metric (CM). Both metrics are of different nature and provide a more accurate prediction in different situations. For MC-SS, where spreading is done, not only the signal metrics must be taken into account but also the multiple access interference (MAI) introduced by the nonlinearity.

There are several strategies to counteract the effect of nonlinearities in multicarrier systems. One way is to linearize the amplifier response at the transmitter so that it resembles as much as possible to a soft limiter. Another solution is to add some signal processing at the receiver side in order to reduce the error rate. The last strategy considered in this thesis consists in reducing the envelope fluctuations of the transmitter signal. In practice this is done by performing PAPR or CM reduction at the transmitter side.

This thesis analyzes the sensitivity of OFDM-based multicarrier systems to nonlinear amplification and looks for efficient ways to reduce it. The thesis is divided into four parts: Overview, Extended analysis and solutions, Concluding remarks and Appendices.

In Part I a general overview of the problem as well as a short description of the best-known compensation techniques is presented. It starts, in Chapter 2, by providing a short overview of the transmission techniques considered in this thesis. Basically, OFDM-based multicarrier communication with possible time and frequency spreading is used. Subsequently, in Chapter 3, a deep study of the power amplifiers used for wireless communication is provided and the well-known mathematical models from the literature for HPA characterization are presented. These concepts are merged in Chapter 4 to evaluate the effects of nonlinear amplifiers in OFDM-based multicarrier systems. As it will be further discussed, the mathematical analysis presented in this chapter is based on the fact that under some circumstances, the OFDM signal can be assumed to be complex-Gaussian distributed. Finally, in Chapter 5, some of the most widely used techniques in the literature that try to compensate the nonlinear distortion effects are described. The overview presented in Part I of this thesis is based on several documents from the literature as well as on some of the contributions that have been done during this PhD.

In Part II a more detailed study of some topics presented in the overview regarding MC and MC-SS systems is done. This part is uniquely based on contributions from the author that have already been published in several journals and conferences or that have recently been submitted for publication. In Chapter 6, a deep study of the effect of nonlinear amplification in OFDM-based multicarrier systems is presented. This includes the extension to non-Gaussian distributed OFDM signals and evaluation of uplink and downlink signals. Moreover, the suitability of both PAPR and CM as different measures of the envelope fluctuations is evaluated. Chapter 7 and Chapter 8 propose two methods based on tone reservation (TR) and controlled spectral outgrowth (CSO), respectively, to reduce the envelope fluctuations of the transmitted OFDM signal. The two methods have low complexity requirements and in both, CM is considered rather than PAPR. Although these solutions are originally designed for OFDM they can also be used in MC-SS systems. Finally, Chapter 9 presents a receiver side strategy for MC-SS systems that aims to reduce the effect of the nonlinear distortion introduced by the transmitter power amplifier (PA). More specifically, in this chapter the implementation of a multiuser detector (MUD) for nonlinearly distorted MC-SS systems is addressed. As it will be shown the proposed MUD always shows better or at least the same performance than conventional MUDs when a nonlinearity is present at the output of the transmitter.

In Part III some conclusions from the presented work are drawn and future research lines are proposed. Finally, in Part IV the reader can find part of the work undertaken at Ericsson Research regarding the uplink of Long Term Evolution (LTE) and the solutions to the mathematical formulations that were derived in previous chapters.

Finally, the reader can find at the end of this thesis the mathematical symbols and definitions, and a list of acronyms.

Chapter 2

Transmission techniques

For the sake of clarity it is important to provide the reader with the definitions, nomenclature and system models considered in the remainder of the thesis. In this chapter a short overview of the transmission techniques is presented. Basically, OFDM-based multicarrier communication with possible time and frequency spreading is used. Many of the definitions and notations included in this chapter will be referenced later to both evaluate the performance of each system when nonlinear amplifiers are present and to formulate efficient compensation techniques.

2.1 Multicarrier communications

Multicarrier transmission is based on splitting a high-rate data stream into many parallel low-rate substreams that are transmitted in different frequency channels, i.e. in different subcarriers [16, 101]. The motivations for using this technique are that no complex equalization is required and high spectral efficiency can be achieved [43,82,98].

Complex equalization is avoided by using many subcarriers with a sufficiently low symbol rate such that the effect of the delay spread decreases significantly. Since the symbol duration of the lower rate subcarriers is increased, the inter-symbol interference (ISI) decreases. Moreover, ISI can be almost eliminated by introducing a guard time in every multicarrier symbol such that the major dispersion in time caused by a multipath channel remains within the guard interval. In the guard time, the multicarrier symbol is cyclically extended to avoid generating inter-carrier interference (ICI). In single-carrier systems ISI occurs and can only be compensated by using complex equalizers at the receiver. In a multicarrier system, no equalization to overcome ISI is required and it is only needed to correct the amplitude and phase of each subcarrier according to the channel frequency response. This is simply done by one complex-valued multiplication per subcarrier, which is in fact a one-tap equalization.

High spectral efficiency is achieved by using a sufficiently large number of subcarri-

ers with a relatively narrow bandwidth each, and by allocating the transmitted power, constellation size and coding rate to each subcarrier efficiently.

Let us evaluate the capacity of a non-ideal linear filter channel to show it. From [82], the capacity of a multicarrier system is

$$C = \int_W \log_2 \left(1 + \frac{P(f)|C(f)|^2}{\Phi_{nn}(f)}\right) df, \tag{2.1}$$

where $C(f)$ is the frequency response of a non-ideal, band-limited channel with bandwidth W, $\Phi_{nn}(f)$ is the power spectral density of the additive Gaussian noise and $P(f)$ represents the distribution of the transmitted signal power in the frequency domain. Note that assuming a nominal average transmitted power P_{av} the following constraint must be fulfilled

$$\int_W P(f)\, df \leq P_{\text{av}}. \tag{2.2}$$

In order to maximize the channel capacity in (2.1) one must compute the optimum distribution of the transmitted signal power. In [82] it is shown that the optimum $P(f)$ is the solution to the equation

$$\frac{1}{P(f) + \Phi_{nn}(f)/|C(f)|^2} + \lambda = 0. \tag{2.3}$$

where λ is a Lagrange multiplier. It can be seen, from (2.3), that $P(f)+\Phi_{nn}(f)/|C(f)|^2$ must be a constant. Therefore, the distribution of the transmitted signal power becomes

$$P(f) = \begin{cases} K - \Phi_{nn}(f)/|C(f)|^2 & \text{if } f \in W \\ 0 & \text{otherwise.} \end{cases} \tag{2.4}$$

where the value of the constant K is adjusted to satisfy the average power constraint in (2.2)

$$K = \frac{1}{W}\left(P_{\text{av}} + \int_W \Phi_{nn}(f)/|C(f)|^2\, df\right). \tag{2.5}$$

From (2.4) one concludes that the power allocated to each subcarrier should be proportional to the channel signal-to-noise ratio (SNR) $|C(f)|^2/\Phi_{nn}(f)$. Moreover the signal in each subcarrier may be independently coded and modulated to increase the spectral efficiency [6, 25, 47, 48]. The above development suggests that properly designed multicarrier modulation systems can achieve transmission rates close to capacity.

OFDM is a low complexity technique to efficiently modulate multiple subcarriers by using digital signal processing [16, 43, 101]. The principle of OFDM is to transmit N distinct substreams over N orthogonal subcarriers. The complex baseband OFDM signal is expressed as

$$s(t) = \frac{1}{\sqrt{N}} \sum_{k=0}^{N-1} S_k e^{j2\pi f_k t}, \qquad 0 \leq t < T_s, \tag{2.6}$$

where S_k is the complex baseband modulated symbol transmitted on the subcarrier at frequency f_k and T_s is the OFDM symbol duration that is determined by the duration of the data symbols, T_d, as

$$T_s = N \cdot T_d. \tag{2.7}$$

In order to satisfy the principle of orthogonality the N subcarriers are located at

$$f_k = \frac{k}{T_s}, \qquad k = 0, 1, \ldots, N-1. \tag{2.8}$$

From (2.6), (2.7) and (2.8) the baseband OFDM signal becomes

$$s(t) = \frac{1}{\sqrt{N}} \sum_{k=0}^{N-1} S_k e^{j2\pi kt/NT_d}, \qquad 0 \leq t < T_s. \tag{2.9}$$

If $s(t)$ is sampled at $t = nT$ we obtain the complex samples as

$$s_n = \frac{1}{\sqrt{N}} \sum_{k=0}^{N-1} S_k e^{j2\pi kn/LN}, \qquad n = 0, 1, \ldots, LN-1, \tag{2.10}$$

where L is the oversampling factor of value

$$L = \frac{T_d}{T}. \tag{2.11}$$

The inverse discrete Fourier transform (IDFT) is given by

$$x_n = \frac{1}{N} \sum_{k=0}^{N-1} X_k e^{j2\pi kn/N}, \qquad n = 0, 1, \ldots, N-1. \tag{2.12}$$

Thus, by zero padding the complex baseband modulated symbol vector of length N with $N(L-1)$ zeros as

$$\mathbf{S}^{\text{zp}} = [S_0, S_1, \ldots, S_{N-1}, \underbrace{0, 0, \ldots, 0}_{N(L-1)}], \tag{2.13}$$

we can reformulate (2.10) to

$$s_n = \frac{1}{\sqrt{N}} \sum_{k=0}^{LN-1} S_k^{\text{zp}} e^{j2\pi kn/LN}, \qquad n = 0, 1, \ldots, LN-1, \tag{2.14}$$

which can be computed by means of a length-LN scaled IDFT of the zero padded complex baseband modulated symbol vector. It can be easily shown that by applying the inverse operation, i.e. a length-LN scaled discrete Fourier transform (DFT) of the OFDM symbol in the time domain, the original sequence S_k can be obtained. This characteristic that allows OFDM to be implemented in the discrete domain by using

IDFT and DFT, or more computationally efficient by using inverse fast Fourier transform (IFFT) and fast Fourier transform (FFT), is another key advantage of OFDM.

Time-domain interpolation consists of two steps: insertion of $(L-1)$ zeros after each sample in the original sequence, where L is the upsampling factor, and low pass filtering the resulting extended sequence. Thus, the vector at the output of the interpolator filter contains the unmodified original samples with $(L-1)$ interpolated values between them. In an OFDM system, interpolation can be done in the frequency domain by zero padding the complex baseband modulated symbol vector before applying the IDFT/IFFT. Zero padding is done by adding the $N(L-1)$ zeros at the end of the complex baseband modulated symbol vector, as in (2.13). However, one should notice that in the complex IFFT, the first half of the samples corresponds to positive frequencies while the last half corresponds to the negative frequencies. Hence, the zeros should be added in the middle of the symbol vector, rather than appending them at the end, as

$$\mathbf{S}^{\text{zp}} = [S_0, \ldots, S_{N/2-1}, \underbrace{0, 0, \ldots, 0}_{N(L-1)}, S_{N/2}, \ldots, S_{N-1}]. \tag{2.15}$$

This ensures that the data bearing subcarriers are placed around 0 Hz at baseband, while zero data values are mapped onto frequencies close to plus and minus half the sampling rate as shown in Figure 2.1.

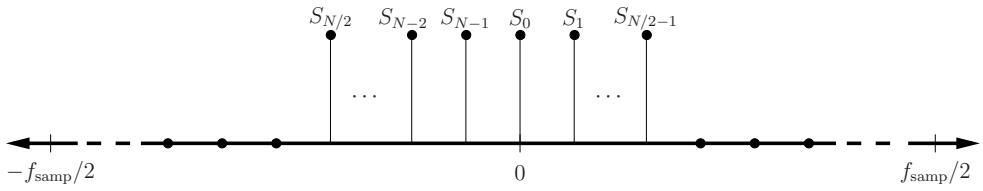

Figure 2.1: Frequency representation of the upsampled OFDM symbols.

The block diagram of a multicarrier system employing an IDFT/IFFT in the OFDM block and a DFT/FFT in the inverse OFDM block is shown in Figure 2.2. At the transmitter side, the input bits are baseband modulated to generate the complex baseband modulated symbols that are driven to the OFDM block, where they are paralleled and optionally zero padded in order to generate the time domain representation of the OFDM symbol by means of the IDFT/IFFT. Subsequently serialization is done and guard time is added at the beginning of each OFDM symbol by cyclically extending the OFDM symbols. In the receiver side, the inverse operation is done to obtain the received information bits.

Advantages and drawbacks of OFDM

Up to now we have seen the motivations for using a multicarrier system based on OFDM. However, such a system has several inherent drawbacks that have to be con-

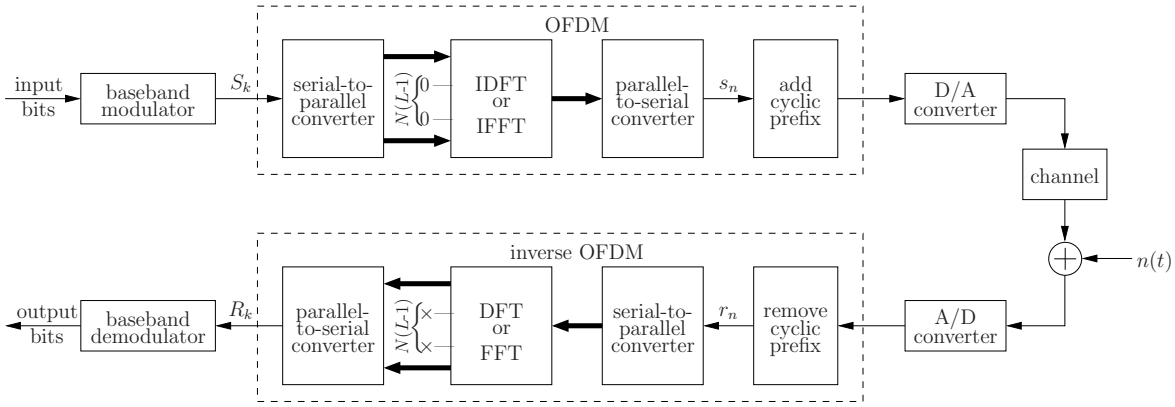

Figure 2.2: Block diagram of an OFDM system.

sidered in the overall design. In the following, the advantages and drawbacks of a multicarrier system based on OFDM are summarized.

Advantages:

- Low computational complexity implementation by means of the FFT operation.
- Robustness against frequency selective fading and time dispersion which allows implementing low computationally complex receivers. Since both ISI and ICI are avoided by using long symbols with sufficiently long cyclic prefix, complex equalization at the receiver side is not necessary.
- Transmission rates close to capacity can be achieved by using a large number of subcarriers with a sufficiently narrow bandwidth each.
- Each substream may be independently coded and modulated according to the transmission conditions on each subcarrier. Thus increasing the spectral efficiency.
- Robustness against narrow-band interference (single-tone interference).
- Flexibility to allocate different users by assigning them different groups of subcarriers, i.e. orthogonal frequency division multiple access (OFDMA).

Drawbacks:

- Sensitivity to frequency offset. If a frequency offset occurs at the input of the OFDM demodulator the bit error-rate (BER) increases drastically since severe ICI occurs due to the overlapping power spectra between neighboring subcarriers. The frequency offset can be either introduced by the channel or by a mismatch in the carrier frequency between the transmitter and receiver local oscillators.

The first implies that OFDM is sensitive to the Doppler spread introduced by the channel, while the second requires accurate frequency synchronization.

- Sensitivity to nonlinear amplification which either requires an inefficient use of power amplifiers or introduces a large performance degradation, i.e. increase of both BER and out-of-band radiation.
- Sensitivity to the resolution and dynamic range of the digital-to-analog (D/A) and analog-to-digital (A/D) converters. Since OFDM suffers from large envelope fluctuations, a high-resolution D/A converter is required at the transmitter and a high-resolution A/D converter operating at high dynamic range is required at the receiver side.
- Loss in power and spectral efficiency due to the guard interval.
- The phase noise introduced by the transmitter and receiver oscillators influences the system performance.
- Accurate time synchronization is required to assure that the FFT window is placed over the useful part of the OFDM symbol discarding the guard interval.

Several disadvantages of using multicarrier modulations based on OFDM have been stated. However, the sensitivity to frequency offset and the sensitivity to nonlinear amplification are pointed out as the major disadvantages of OFDM.

2.2 Spread-spectrum communications

Spread-spectrum (SS) is based on spreading the transmitted signal over a frequency band much wider than the one required to transmit the information being sent. At the receiver, synchronizing the received signal is necessary for despreading and, thus, recover the data signal. Even though the initial applications of spread-spectrum systems mainly exploited the antijamming and low probability of interception characteristics for military communications, robustness to multipath and multiple access suggested that spread-spectrum was used in commercial systems.

There are two main techniques for applying the concept of spread-spectrum: direct-sequence (DS) and frequency-hopping (FH). The idea behind DS-SS is to multiply the data being transmitted by a pseudo-random (PN) sequence at a frequency much higher than that of the original signal. The pseudo-random sequence, which is independent of the data, is known as *spreading code* and the elements constituting the spreading code are denoted as *chips*. In a multiuser environment, the user signals are distinguished by different PN codes so that all signals can be transmitted in the same time and frequency channel. This principle of user separation is referred to as code division multiple access (CDMA) and in the particular case where DS-SS is used it is known as

DS-CDMA. FH-SS is similar to DS-SS in the sense that a pseudo-random sequence is used to spread the signal over a much larger bandwidth. However, instead of spreading the signal over a continuous bandwidth by mixing the signal with the spreading code, the signal bandwidth is unchanged and hopped over a large number of channels of the same bandwidth as the transmitted signal.

2.3 Multicarrier spread-spectrum communications

The success of spread-spectrum in mobile communications and OFDM in digital broadcasting and wireless LANs motivated many researchers to investigate on the combination of both techniques. In the same way that in multicarrier systems two dimensions can be used to allocate the different data symbols: time and frequency, in a MC-SS system the chips of the spread data symbols can be mapped in both time and frequency dimensions. When allocation is done in the frequency domain, the system is referred to as MC-CDMA. On the other hand, when allocation is done in the time domain, it is termed as MC-DS-CDMA. A more general system where allocation is considered in both time and frequency domains is known as orthogonal frequency and code division multiple access (OFCDMA).

MC-CDMA

A general view of a MC-CDMA system is shown in Figure 2.3. Here, K data streams (which might belong to different users and applications) are spread by using stream-specific spreading codes and transmitted on several narrow-band subcarriers. Multicarrier modulation is done by using the low-complex OFDM operation. The major characteristic of such systems is that since spreading is done in the frequency domain, a high frequency diversity gain is achieved. MC-CDMA offers several advantages and drawbacks when considered in the uplink and downlink of mobile radio systems. However, providing a detailed study of such schemes falls beyond the scope of this thesis. Therefore, the reader is referred to [43] for further information.

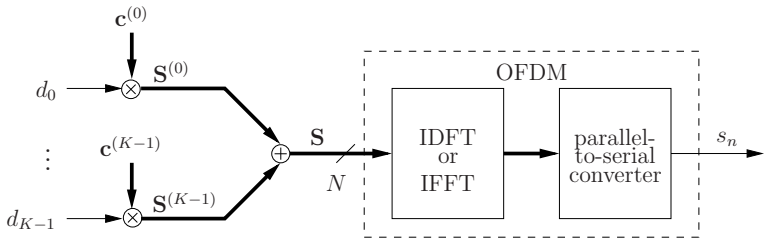

Figure 2.3: General view of a MC-CDMA system.

One should note that in the general view of a MC-CDMA system illustrated in

Figure 2.3, a downlink transmission is assumed since the data streams might belong to different users. In fact, the scheme for the uplink is very similar to that in Figure 2.3 but only the data streams of the corresponding user are transmitted. Another important difference between downlink and uplink MC-CDMA systems is the type of spreading codes used. In the downlink, where synchronous transmission is done, orthogonal spreading codes have the advantage of reducing MAI compared to non-orthogonal ones. In the uplink, the orthogonality between the spreading codes is generally lost and, hence, simple PN sequences can be chosen. However, in the synchronous uplink orthogonal codes are shown to still outperform non-orthogonal ones [43]. Another important aspect to notice in Figure 2.3 is that it is assumed that the spreading code length L_{sc} is equal to the number of subcarriers N. One disadvantage of such assumption is that for large number of subcarriers the spreading code becomes unnecessarily large and no more frequency diversity is gained compared to shorter spreading sequences, while higher MAI is introduced in heavily loaded systems. Nevertheless, the flexibility offered by a MC-CDMA system allows finding efficient solutions that not only introduce flexibility to the system design, but can also reduce the complexity of the receiver. Among the variety of solutions in the literature the two most widely accepted schemes are known as spread-spectrum multicarrier multiple access (SS-MC-MA) and group orthogonal MC-CDMA (GO-MC-CDMA).

In SS-MC-MA the total number of subcarriers N is uniformly divided among K users, resulting in $N/K = L_{\text{sc}}$ subcarriers per user. Then, each user maps M data symbols to the L_{sc}-subcarrier subsystem which is exclusively assigned to this user. Each data symbol is spread by means of a spreading code of length L_{sc}. Therefore, OFDMA is used for user separation and CDM is used to transmit the different data symbols belonging to the same user. The major characteristic of this scheme is that since OFDMA is used no MAI occurs. On the other hand, SS-MC-MA systems have to cope with self interference caused by the superposition of signals from the same user. A general view of a downlink SS-MC-MA system is shown in Figure 2.4. As in MC-CDMA the uplink system is very similar to that of the downlink but only the data symbols of the corresponding user are transmitted, thus occupying only L_{sc} subcarriers from the total N subcarriers. The reader is referred to [43] for further information.

As shown in Figure 2.5, in GO-MC-CDMA the total number of subcarriers N is uniformly divided among M user groups, i.e. $N/M = L_{\text{sc}}$ subcarriers per group. The user group is constituted by all the K users in the GO-MC-CDMA system in such a way that each user exploits all the M groups to transmit M data symbols, that is, one data symbol per group. Therefore, in GO-MC-CDMA, OFDM is used to separate the different user data symbols and CDMA to separate the different users that share the same transmission bandwidth. In opposite to SS-MC-MA MAI occurs but no self interference among different data symbols of the same users exists. The reader is referred to [22] for further information.

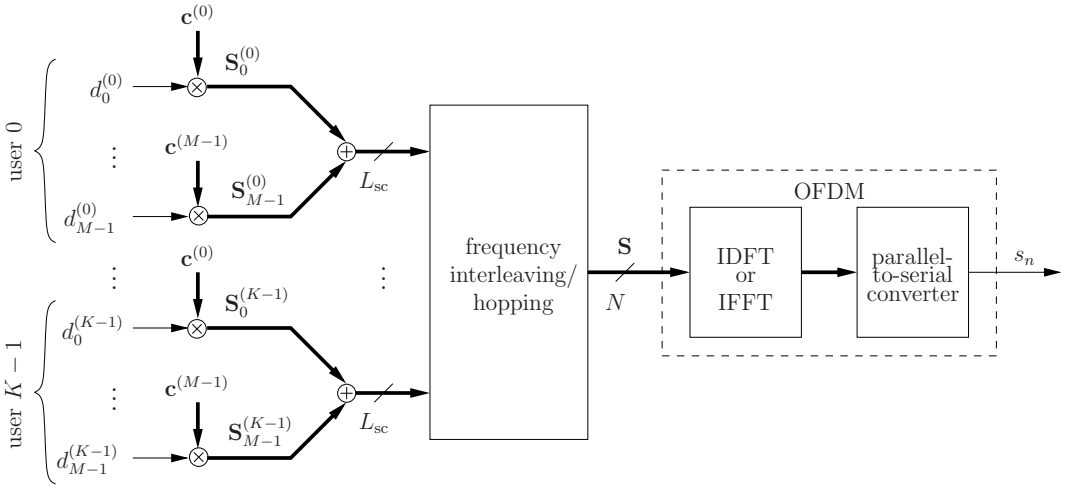

Figure 2.4: General view of a SS-MC-MA system.

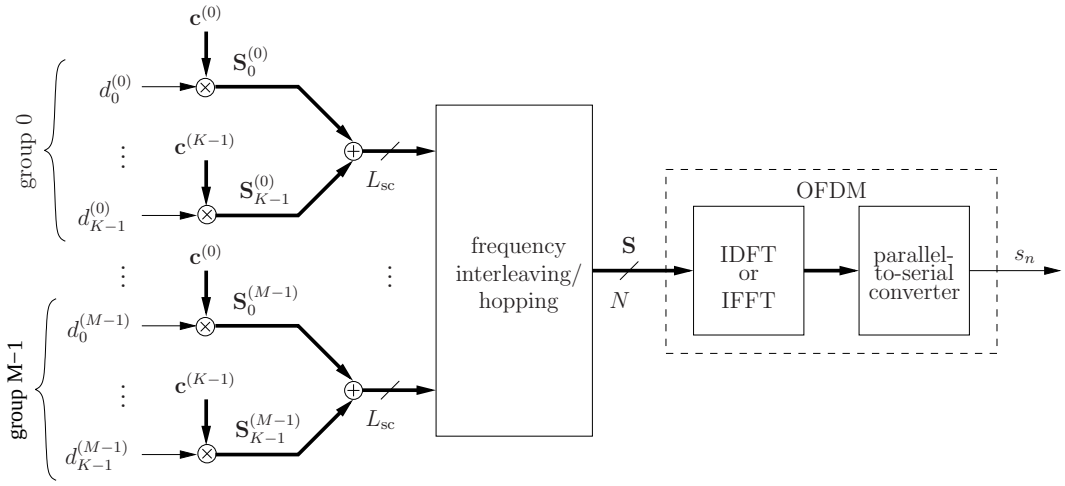

Figure 2.5: General view of a GO-MC-CDMA system.

MC-DS-CDMA

MC-DS-CDMA can be seen as N DS-CDMA systems transmitting over N distinct subcarriers, thus, if only one subcarrier is used MC-DS-CDMA is identical to single-carrier DS-CDMA. An advantage of MC-DS-CDMA compared to single-carrier DS-CDMA is that due to multicarrier transmission complex equalization at the receiver side is not necessary. A general view of a MC-DS-CDMA system is shown in Figure 2.6. As it can be observed M data symbols are spread by using M different spreading codes and transmitted over a single subcarrier. The resulting sequence of chips, of length L_{sc}, is transmitted consecutively in time on the same subcarrier, thus occupying L_{sc} OFDM symbols.

MC-DS-CDMA is of special interest for the asynchronous uplink of mobile radio systems due to its close relation to asynchronous single-carrier DS-CDMA systems. Thus, as in the latter, spreading codes with good auto-correlation and cross-correlation properties, such as PN or Gold codes, are preferable. For the downlink, orthogonal codes are used. The major characteristic of MC-DS-CDMA is that since the chips of the spread data symbols are allocated in time domain a high time diversity is achieved. Again, providing a detailed study of such systems falls beyond the scope of this thesis and, therefore, the reader is referred to [43] for further information.

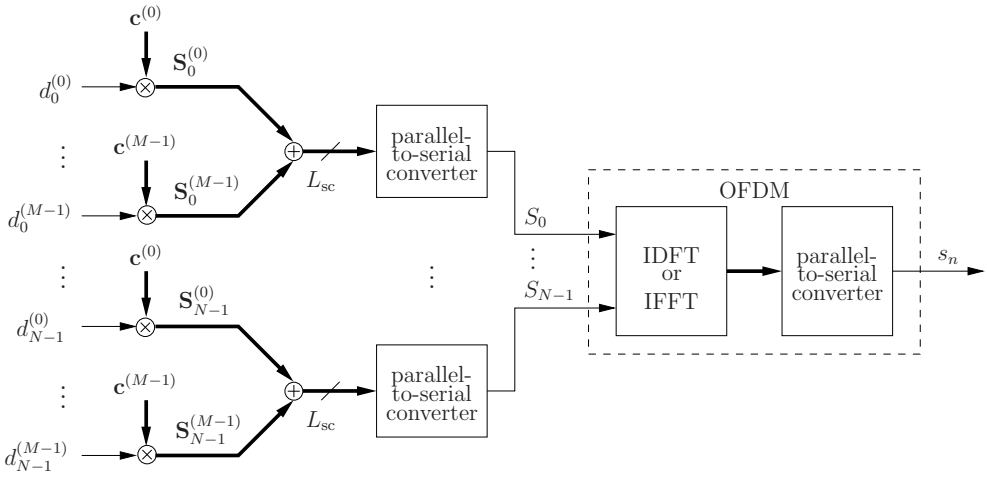

Figure 2.6: General view of a MC-DS-CDMA system.

OFCDMA

An OFCDMA system can be understood as the general case of MC-SS where spreading is possible in both time and frequency domains, resulting in both time and frequency diversity. In the block diagram of Figure 2.7 it is depicted how before the OFDM block each data symbol is spread and the corresponding chips are allocated in a time-frequency grid, denoted as framing. In an adaptive implementation the length of the spreading code is not necessarily fixed but it can be chosen according to transmission rate and channel requirements, this is referred to as variable spreading factor (VSF). The reader is referred to [9] for further information.

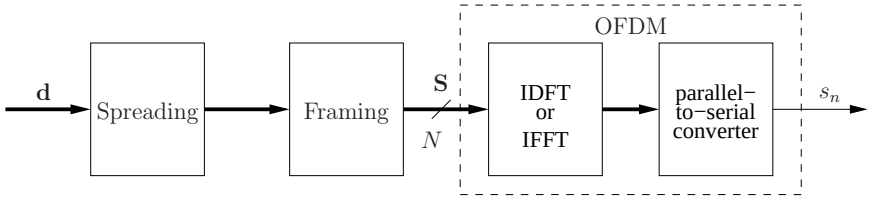

Figure 2.7: General view of an OFCDMA system.

Chapter 3

Nonlinear models for high power amplifiers

This chapter provides a study of the power amplifiers used for wireless communication and presents the well known mathematical models for HPA characterization from the literature. The HPA models presented in this chapter will be used in subsequent chapters to evaluate the performance of OFDM-based multicarrier systems. In order to demonstrate the validity of the classical models we will start by presenting an analytical formulation, based on the Volterra series, of a nonlinear device. In the end of the chapter, the mathematical definitions used to specify the operating point of a power amplifier will be presented.

Two major types of power amplifiers are used in communication systems, traveling wave tube amplifiers (TWTA) and solid state power amplifiers (SSPA). A common characteristic of both devices is that the signal at their output is a nonlinear function of the input signal at both the present and previous instants. Note that the dependence on the value of the input signal at previous instants can be interpreted as memory. Therefore, roughly speaking, one can define high power amplifiers as nonlinear operators with memory.

It is easy to see that high power amplifiers have a nonlinear response, however, it is not obvious why they show a memory effect. It has been shown that memory is mainly due to electrical and electro-thermal effects in the real device [17, 18, 100]. Both electrical and electro-thermal effects are frequency-dependent. This frequency-dependent behavior can be modeled by a filter (whose output signal depends on the input signal at both the present and previous instants), which is a device with memory.

To understand the electrical effect first note that the terminal impedance consists of two parts: the internal impedance of the amplifying device (e.g. a transistor) and the external impedance. The external impedance also comprises two parts: the impedance of the matching network and the impedance of the bias network. The predominant fac-

tor that causes the electrical memory effect is the variation of the terminal impedances (matching and biasing networks) over the input signal bandwidth.

The thermal memory effects are caused by electro-thermal couplings as it is subsequently described. The instantaneous temperature of the power amplifying device is determined by the sum of three components: the ambient temperature, the thermal resistance multiplied by the continuous (dc) power dissipation and the thermal impedance multiplied by the instantaneous power of the transmitted signal. The thermal impedance represents the temperature variations in the high power amplifier that are caused by the dissipated power. This thermal impedance has a purely resistive term (denoted as thermal resistance) that is frequency-independent and a frequency-dependent capacitive term. Since the thermal impedance is frequency-dependent, the third term that determines the instantaneous temperature of the power amplifying device changes with the input signal frequency. Moreover, since the instantaneous gain of the amplifier is a function of its instantaneous temperature, and this is frequency dependent, one concludes that the gain of the amplifier depends on the frequency of the input signal. Note that in order to avoid memory effects both the terminal and thermal impedances should be constant over the input signal bandwidth. However, since this frequency dependence is unavoidable, the memory effect can only be avoided by using a sufficiently narrow signal bandwidth.

The response of a linear system with memory is commonly described by the convolution of the input signal with the system's response to a Dirac delta function, i.e. the impulse response,

$$y(t) = \int_{-\infty}^{\infty} h(\tau)x(t-\tau)d\tau, \tag{3.1}$$

where $x(t)$ and $y(t)$ are the input and output signals, respectively, and $h(t)$ is the impulse response of the system. On the other hand, a nonlinear system without memory can be described by a Taylor series of the form

$$y(t) = \sum_{n=0}^{\infty} a_n \left(x(t)\right)^n \tag{3.2}$$

where a_n denote the coefficients of the series. The Volterra series is a generalization of the Taylor series that also takes into account the system memory by means of

convolution as

$$\begin{aligned} y(t) &= \sum_{n=0}^{\infty} \int_{-\infty}^{\infty} d\tau_1 \int_{-\infty}^{\infty} d\tau_2 \cdots \int_{-\infty}^{\infty} d\tau_n h_n(\tau_1, \tau_2, \ldots, \tau_n) \prod_{i=1}^{n} x(t-\tau_i) \\ &= h_0 + \int_{-\infty}^{\infty} d\tau_1 \; h_1(\tau_1) x(t-\tau_1) \\ &+ \int_{-\infty}^{\infty} d\tau_1 \int_{-\infty}^{\infty} d\tau_2 \; h_2(\tau_1, \tau_2) x(t-\tau_1) x(t-\tau_2) \\ &+ \int_{-\infty}^{\infty} d\tau_1 \int_{-\infty}^{\infty} d\tau_2 \int_{-\infty}^{\infty} d\tau_3 \; h_3(\tau_1, \tau_2, \tau_3) x(t-\tau_1) x(t-\tau_2) x(t-\tau_3) \\ &+ \ldots \end{aligned} \tag{3.3}$$

where $h_n(\tau_1, \cdots, \tau_n)$ is the n-th order impulse response of the system. The functions $\{h_0, h_1(\tau_1), h_2(\tau_1, \tau_2), \ldots\}$ are called the Volterra kernels of the system. The zeroth-order term accounts for the DC component. The first-order kernel is the linear impulse response of the system, i.e. the linear amplification of the input signal, while the higher-order kernels ($n \geq 2$) can be considered as multidimensional impulse responses of the system that characterize the nonlinearities introduced by the HPA. Without any assumption on the nature of the kernels, the computation necessary to produce an output sample from the n-th kernel is the number of operations required for $n = 1$, raised to the n-th power. Thus it is clear that unless the series can be truncated at some fairly small number of terms, the computational load will quickly become too large [57]. For modeling real devices, the Volterra kernels have to be causal for all n

$$h_n(\tau_1, \cdots, \tau_n) = 0 \; \forall \; \tau_i < 0, \; i = 1, 2, \ldots, n. \tag{3.4}$$

Although Volterra series is the most general model to describe all different types of nonlinearities, it is said to be impractical due to the high computational complexity required and the difficulty of finding the kernels of the series. Another problem, is justifying the truncation of the series [57]. For these reasons, several low-complexity models, denoted as high-level models, have been developed to describe the behavior of nonlinear devices [5, 45, 85–87].

In the remainder of this chapter several models for nonlinearities with memory [5,87] and without memory [45, 85, 86] are presented.

3.1 Memoryless models

The behavior of memoryless models can be obtained as a special case of the Volterra series in (3.3) where the output at any time is only dependent on the input value at the same instant. In the following the Volterra series will be simplified to consider only

a memoryless nonlinearity. Subsequently, by analyzing the resulting mathematical expression we will be able to introduce the high-level models that are commonly used in the literature.

Let us first introduce some basic definitions and approximations that are commonly used in the analysis of communication systems. Many digital information-bearing signals are transmitted using some type of carrier modulation. The channel over which the signal is transmitted is limited in bandwidth to an interval of frequencies centered around the carrier [82]. When the bandwidth of the channel is much smaller than the carrier frequency, it is said to be a narrow-band bandpass channel. In the same way, if the bandwidth of a signal is much smaller than its carrier frequency,

$$B_x \ll f_c, \tag{3.5}$$

the signal is said to be a narrow-band bandpass signal. Where B_x is the bandwidth of the bandpass signal $x(t)$ and f_c is the carrier frequency. The bandpass signal is generated at the transmitter side from a frequency translation of the equivalent baseband signal. At the receiver, frequency translation to obtain the baseband equivalent of the received bandpass signal is done prior to the demodulation stage. Baseband equivalence is required for real time digital signal processing and to reduce the simulation time. Therefore, it is desirable to have a mathematical formulation that reduces all bandpass signals to equivalent low pass signals. Let $x_b(t)$ be the equivalent baseband of $x(t)$ expressed in the polar coordinate system expression as

$$x_b(t) = u_x(t)e^{j\alpha_x(t)} \tag{3.6}$$

then the relation between the bandpass signal $x(t)$ and its baseband equivalent $x_b(t)$ is

$$x(t) = \mathrm{Re}\{x_b(t)e^{jw_ct}\} = \frac{1}{2}x_b(t)e^{jw_ct} + \frac{1}{2}x_b^*(t)e^{-jw_ct}, \tag{3.7}$$

where $w_c = 2\pi f_c$.

Let us now assume that the time span of any component of the Volterra kernels, $|\tau_i|;\ \forall\ i = 1, 2, \ldots, n$, is much shorter than the inverse of the bandwidth of the input baseband signal, i.e.

$$|\tau_i| \ll \frac{1}{B_x} \qquad i = 1, 2, \ldots, n. \tag{3.8}$$

In this case, the Volterra kernels can be approximated as multidimensional delta functions $\delta(\tau_1, \ldots, \tau_m)$ and, as a result, it can be assumed that

$$x_b(t - \tau_i) \approx x_b(t) \qquad \forall\ |\tau_i| \ll \frac{1}{B_x} \tag{3.9}$$

which leads us to a memoryless approximation with regard to the baseband equivalent of the nonlinear system [39]. Note that the equivalent approximation in the passband phase component,

$$e^{jw_c(t-\tau_i)} \approx e^{jw_ct}, \tag{3.10}$$

is not valid since the phase term introduced by $w_c\tau_i$ can not be neglected [39].

By using the above considerations, the general Volterra series defined in (3.3) can be particularized to model a memoryless, narrow-band, bandpass system as

$$\begin{aligned}
y(t) &= \sum_{n=0}^{\infty} \int_{-\infty}^{\infty} d\tau_1 \cdots \int_{-\infty}^{\infty} d\tau_n h_n(\tau_1, \ldots, \tau_n) \prod_{i=1}^{n} \mathrm{Re}\{x_b(t) e^{jw_c(t-\tau_i)}\} \\
&= \sum_{n=0}^{\infty} \int_{-\infty}^{\infty} d\tau_1 \cdots \int_{-\infty}^{\infty} d\tau_n h_n(\tau_1, \ldots, \tau_n) \prod_{i=1}^{n} \mathrm{Re}\{u_x(t) e^{j[w_c(t-\tau_i)+\alpha_x(t)]}\} \\
&= \sum_{n=0}^{\infty} \int_{-\infty}^{\infty} d\tau_1 \cdots \int_{-\infty}^{\infty} d\tau_n h_n(\tau_1, \ldots, \tau_n) \left(\frac{u_x(t)}{2}\right)^n \times \\
&\quad \times \prod_{i=1}^{n} \left(e^{j[w_c(t-\tau_i)+\alpha_x(t)]} + e^{-j[w_c(t-\tau_i)+\alpha_x(t)]}\right) \qquad (3.11) \\
&= \sum_{n=0}^{\infty} \int_{-\infty}^{\infty} d\tau_1 \cdots \int_{-\infty}^{\infty} d\tau_n h_n(\tau_1, \ldots, \tau_n) \left(\frac{u_x(t)}{2}\right)^n \times \\
&\quad \times \sum_{l=0}^{n} \sum_{m=1}^{\binom{n}{l}} e^{j\left[\left(n-2l\right)\left(w_c t+\alpha_x(t)\right)+w_c\Theta(l,m)\right]}. \qquad (3.12)
\end{aligned}$$

The product of the n complex conjugated terms in (3.11) has been equivalently expressed as a double sum in (3.12). This will allow us to discard the high order terms that correspond to the harmonics and, therefore, just consider the signal that is around the carrier frequency. The parameter $\Theta(l, m)$ stands for the summation $\sum_{i=1}^{n}(\pm)\tau_i$, where the sign of τ_i depends on the combination of l conjugated elements and $n - l$ non-conjugated elements defined for each term indexed by m [39, 57].

Example 1
To see the equivalence between (3.11) *and* (3.12) *let us consider the* $n = 2$ *case. The complex conjugated terms in* (3.11)*, denoted as A, are*

$$\begin{aligned}
A &= \prod_{i=1}^{2} \left(e^{j[w_c(t-\tau_i)+\alpha_x(t)]} + e^{-j[w_c(t-\tau_i)+\alpha_x(t)]}\right) \\
&= e^{j[w_c(t-\tau_1)+\alpha_x(t)+w_c(t-\tau_2)+\alpha_x(t)]} + e^{j[w_c(t-\tau_1)+\alpha_x(t)-w_c(t-\tau_2)-\alpha_x(t)]} + \\
&\quad + e^{j[-w_c(t-\tau_1)-\alpha_x(t)+w_c(t-\tau_2)+\alpha_x(t)]} + e^{j[-w_c(t-\tau_1)-\alpha_x(t)-w_c(t-\tau_2)-\alpha_x(t)]} \\
&= e^{j[2(w_c t+\alpha_x(t))+w_c(-\tau_1-\tau_2)]} + e^{j[w_c(-\tau_1+\tau_2)]} + e^{j[w_c(\tau_1-\tau_2)]} + \\
&\quad + e^{j[-2(w_c t+\alpha_x(t))+w_c(\tau_1+\tau_2)]}. \qquad (3.13)
\end{aligned}$$

Now, let us expand the equivalent double sum in (3.12)*, denoted as* B*,*

$$\begin{aligned} B &= \sum_{l=0}^{2}\sum_{m=1}^{\binom{2}{l}} e^{j\Big[\big(n-2l\big)\big(w_c t+\alpha_x(t)\big)+w_c\Theta(l,m)\Big]} \\ &= \underbrace{e^{j[2(w_c t+\alpha_x(t))+w_c\Theta(0,1)]}}_{l=0} + \underbrace{e^{j[w_c\Theta(1,1)]}+e^{j[w_c\Theta(1,2)]}}_{l=1} + \underbrace{e^{j[-2(w_c t+\alpha_x(t))+w_c\Theta(2,1)]}}_{l=2}, \end{aligned} \tag{3.14}$$

By comparing (3.13) *and* (3.14) *one can see that both expressions are, in fact, equivalents, with* $\Theta(0,1)=-\tau_1-\tau_2$*,* $\Theta(1,1)=-\tau_1+\tau_2$*,* $\Theta(1,2)=\tau_1-\tau_2$*,* $\Theta(2,1)=\tau_1+\tau_2$*. Which can be expressed in a general form as* $\sum_{i=1}^{2}(\pm)\tau_i$*.*

From (3.12), it can be see that when a bandpass signal is driven to a nonlinear device, harmonics at the $(n-2l)$ multiples of the carrier frequency will appear at the output of the nonlinearity. Although this could be used to predict the harmonic levels, in this thesis we are just interested in the signal around the carrier frequency. The zone located around the carrier frequency is referred to as the first-zone, and the signal therein as the first-zone signal. The first-zone signal from (3.12) can be obtained by taking

$$(n-2l)=\pm 1. \tag{3.15}$$

Notice that (3.15) only holds for odd values of n, which matches with the fact that only odd power nonlinearity terms contribute to the first-zone of a nonlinear bandpass system [57]. The even order terms generate spectral components at least f_c away from the carrier frequency. From (3.12) and (3.15), the first-zone signal at the output of the nonlinearity becomes

$$\begin{aligned} y_1(t) = \sum_{n=1}^{\infty}\int_{-\infty}^{\infty} d\tau_1\cdots\int_{-\infty}^{\infty} d\tau_n h_n(\tau_1,\ldots,\tau_n)\left(\frac{u_x(t)}{2}\right)^n \times \\ \times \sum_{l=\frac{n\mp1}{2}}\sum_{m=1}^{\binom{n}{l}} e^{j\Big[\big(n-2l\big)\big(w_c t+\alpha_x(t)\big)+w_c\Theta(l,m)\Big]} \end{aligned} \tag{3.16}$$

where $n=1,3,5,7,\ldots$. Since l takes only two values, i.e. $l=\frac{n-1}{2}$ and $l=\frac{n+1}{2}$, $\binom{n}{l}$ can be rewritten as two different terms: $\binom{n}{\frac{n-1}{2}}$ and $\binom{n}{\frac{n+1}{2}}$. It is interesting to notice that

$$\binom{n}{\frac{n-1}{2}} = \frac{n!}{\frac{n-1}{2}!\frac{n+1}{2}!} = \binom{n}{\frac{n+1}{2}}, \tag{3.17}$$

so we define

$$C_{(n)} = \binom{n}{\frac{n\mp1}{2}}. \tag{3.18}$$

Additionally, since

$$\Theta\left(\frac{n+1}{2},m\right) = -\Theta\left(-\frac{n+1}{2},m\right) \qquad 1\le m\le C_{(n)} \tag{3.19}$$

one can rewrite the bandpass first-zone signal at the output of the nonlinearity in (3.16) as

$$\begin{aligned} y_1(t) &= \sum_{n=1}^{\infty} \int_{-\infty}^{\infty} d\tau_1 \cdots \int_{-\infty}^{\infty} d\tau_n h_n(\tau_1, \ldots, \tau_n) \left(\frac{u_x(t)}{2}\right)^n 2\,\mathrm{Re}\left\{ \sum_{m=1}^{C_{(n)}} e^{j\left[w_c t + \alpha_x(t) + w_c \Theta\left(\frac{n+1}{2}, m\right)\right]} \right\} \\ &= \mathrm{Re}\Bigg\{ \sum_{n=1}^{\infty} \Bigg[\underbrace{\Bigg[\int_{-\infty}^{\infty} d\tau_1 \cdots \int_{-\infty}^{\infty} d\tau_n 2\, h_n(\tau_1, \ldots, \tau_n) \sum_{m=1}^{C_{(n)}} e^{j\left[w_c \Theta\left(\frac{n+1}{2}, m\right)\right]} \Bigg]}_{K_n} \left(\frac{u_x(t)}{2}\right)^n \Bigg] \times \\ &\qquad \times e^{j\alpha_x(t)} e^{j w_c t} \Bigg\} \\ &= \mathrm{Re}\left\{ \left[\sum_{n=1}^{\infty} K_n \left(\frac{u_x(t)}{2}\right)^n \right] e^{j\alpha_x(t)} e^{j w_c t} \right\} \end{aligned} \tag{3.20}$$

The term K_n is independent of the input signal and only describes the behavior of the nonlinearity. Notice that $\sum_{n=1}^{\infty} K_n \left(\frac{u_x(t)}{2}\right)^n$ is a complex value that for a given nonlinearity (i.e. for a given K_n), just depends on $\left(\frac{u_x(t)}{2}\right)^n$, i.e. the envelope of the input signal. As a result, one can write

$$\sum_{n=1}^{\infty} K_n \left(\frac{u_x(t)}{2}\right)^n = G\big(u_x(t)\big) e^{j\Phi\left(u_x(t)\right)}. \tag{3.21}$$

By substituting (3.21) into (3.20) one obtains

$$y_1(t) = \mathrm{Re}\left\{ G\big(u_x(t)\big) e^{j\left[\alpha_x(t) + \Phi\left(u_x(t)\right)\right]} e^{j w_c t} \right\}, \tag{3.22}$$

which represents a bandpass signal of the form

$$y_1(t) = \mathrm{Re}\left\{ u_{y_1}(t) e^{j\alpha_{y_1}(t)} e^{j w_c t} \right\}. \tag{3.23}$$

Hence, the amplitude of the output signal of the nonlinearity is only a function of the input amplitude. The conversion from the input amplitude to the output amplitude is referred to as amplitude modulation to amplitude modulation (AM/AM) and is represented by the function $G(\cdot)$. On the other hand the phase of the output signal is equal to the phase of the input signal plus a distortion term that depends on the input amplitude. The conversion from the input amplitude to the output phase is known as amplitude modulation to phase modulation (AM/PM) and is represented by the function $\Phi(\cdot)$.

The baseband modeling of a memoryless nonlinearity is depicted in Figure 3.1. The time dependency has been removed since $G(\cdot)$ and $\Phi(\cdot)$ only rely on the present value of the input signal envelope.

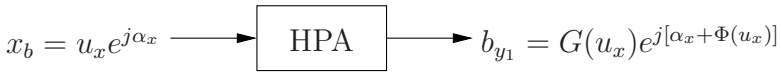

Figure 3.1: Baseband modeling of memoryless nonlinearities.

The baseband modeling of memoryless nonlinearities depicted in Figure 3.1 was first obtained by experimental observation [14]. An important aspect is how the AM/AM and AM/PM characteristics are represented. Since we aim at modeling a real nonlinear amplifier, we can think of constructing large look up tables and interpolating to obtain the remaining values. An alternative is to use analytical representation of the real nonlinear characteristic. In analytical representation, a general AM/AM function, $G(\cdot)$ and a general AM/PM function, $\Phi(\cdot)$ are used to approximate the nonlinearity response. This is done by setting the coefficients in $G(\cdot)$ and $\Phi(\cdot)$ so that a least-squares approximation is achieved. Several AM/AM and AM/PM functions can be found in the literature, such as the one proposed by Saleh [86], Rapp [85] and Ghorbani [45].

Saleh model

The Saleh model [86] is commonly used for traveling-wave tube power amplifiers. Its AM/AM and AM/PM conversion functions are:

$$\text{AM/AM: } G(u_x) = \frac{\kappa_G \cdot u_x}{1 + \chi_G \cdot u_x^2}, \tag{3.24}$$

$$\text{AM/PM: } \Phi(u_x) = \frac{\kappa_\Phi \cdot u_x^2}{1 + \chi_\Phi u_x^2}. \tag{3.25}$$

An example of the AM/AM and AM/PM characteristics that can be obtained by the Saleh model is depicted in Figure 3.2. It has been obtained by setting $\kappa_G = 2$, $\chi_G = \chi_\Phi = 1$ and $\kappa_\Phi = \pi/3$.

Rapp model

The Rapp [85] model is used for modeling solid state power amplifiers. Its AM/AM and AM/PM conversion functions are determined by

$$\text{AM/AM: } G(u_x) = \frac{\kappa_G \cdot u_x}{(1 + (\frac{u_x}{O_{sat}})^{2s})^{\frac{1}{2s}}}, \tag{3.26}$$

$$\text{AM/PM: } \Phi(u_x) = 0, \tag{3.27}$$

where s is the smoothness factor and O_{sat} is the output saturation level. Note that since the output phase is not affected, this represents a truly memoryless model. Figure 3.3 shows an example of the AM/AM characteristic that can be obtained by the Rapp model. This characteristic has been obtained by setting $\kappa_G = O_{sat} = 1$ and $s = 3$.

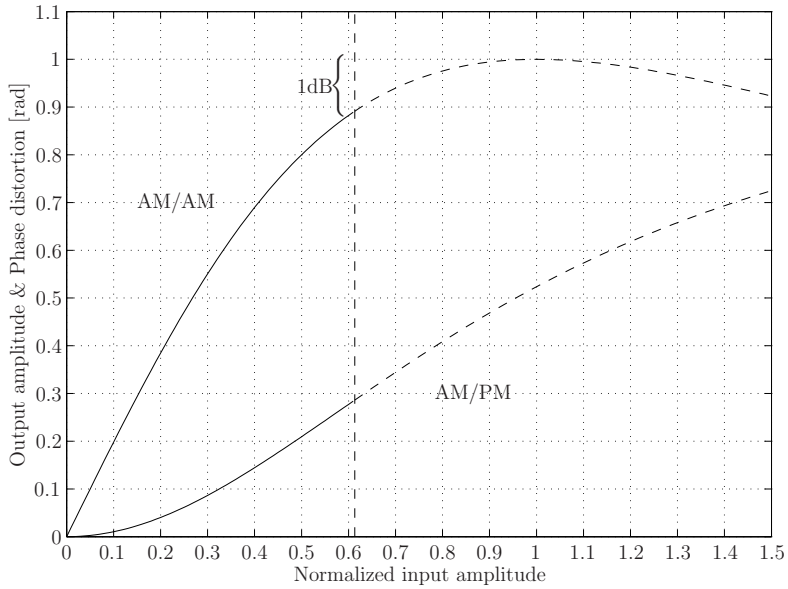

Figure 3.2: Example of the AM/AM and AM/PM characteristics of Saleh model.

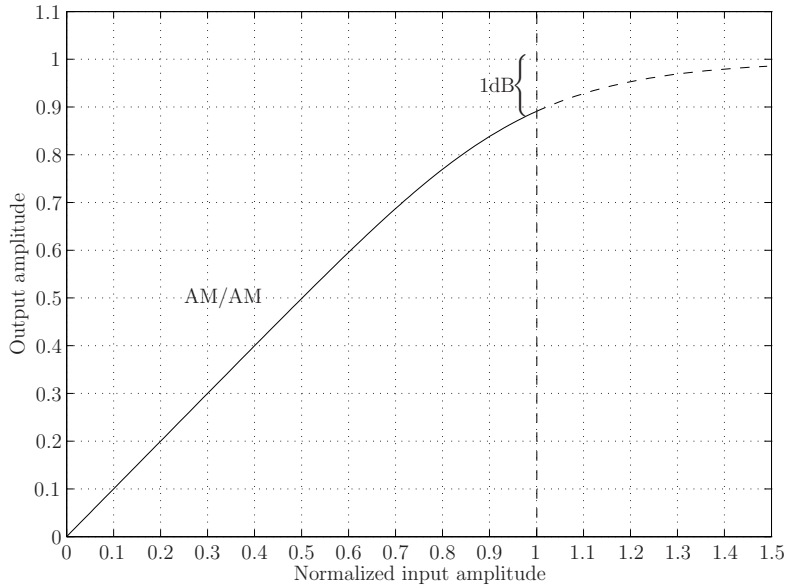

Figure 3.3: Example of the AM/AM (AM/PM is 0) characteristic of Rapp model.

Ghorbani model

The Ghorbani model [45] is also used for modeling solid state power amplifiers. Its AM/AM and AM/PM conversion functions are:

$$\text{AM/AM: } G(u_x) = \kappa_{G_1} \cdot u_x + \frac{\kappa_{G_2} \cdot {u_x}^{n_G}}{1 + \chi_G \cdot {u_x}^{n_G}}, \tag{3.28}$$

$$\text{AM/PM: } \Phi(u_x) = \kappa_{\Phi_1} \cdot u_x + \frac{\kappa_{\Phi_2} \cdot {u_x}^{n_\Phi}}{1 + \chi_\Phi \cdot {u_x}^{n_\Phi}}. \tag{3.29}$$

An example of the AM/AM and AM/PM characteristics that can be obtained by the Ghorbani model is depicted in Figure 3.4. It has been obtained by setting $\kappa_{G_1} = 0$, $\kappa_{G_2} = \chi_G = 20$, $n_G = n_\Phi = 2$, $\kappa_{\Phi_1} = \pi/15$, $\kappa_{\Phi_2} = \pi/3$ and $\chi_\Phi = \pi$.

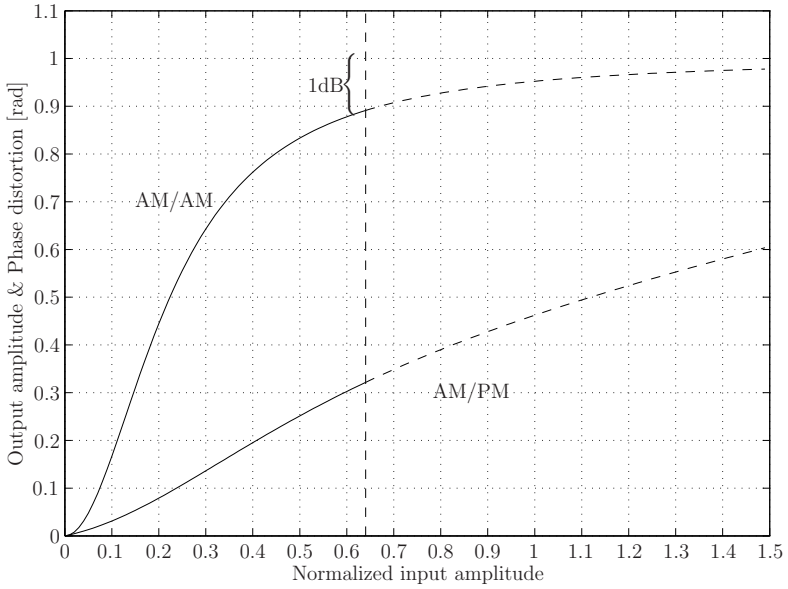

Figure 3.4: Example of the AM/AM and AM/PM characteristics of Ghorbani model.

3.2 Models with memory

In the previous section, models for memoryless nonlinearities were discussed. The theoretical analysis from Volterra series that led to the definition of the AM/AM and AM/PM characteristics was derived by assuming that the bandwidth of the signal was much smaller than the bandwidth of the nonlinearity, i.e. that a narrow-band signal was used. Under this assumption it was found out that the effect of a memoryless nonlinearity over the output signal amplitude and phase just relies on the present value of the input amplitude. This suggests that the model is frequency independent. If one used the so-called memoryless models to characterize the effect of nonlinear devices in

wideband signals, by which it means that the bandwidth of the signal is comparable to the inherent bandwidth of the device, one would see that all frequencies are equally distorted. However, from real measurements it is known that real power amplifiers are frequency dependent. In short, memoryless models are only suitable for narrow-band signals since over any relatively small portion of the band, the transfer characteristic looks nearly frequency independent.

A frequency-dependent behavior can be obtained by introducing memory to the model. In a nonlinear model with memory the output signal depends on the value of the input signal at both present and previous instants.

The most general way to describe a nonlinear system with memory is by using the Volterra series in (3.3). However, as discussed previously, they are impractical due to the high computational complexity. Also it is difficult both to determine the kernels of the series and to justify its truncation. A less complex solution is obtained by introducing a filter to the memoryless nonlinear models described previously. The Hammerstein, the Wiener and the Filter-Nonlinearity-Filter models are three examples of such solution.

The Hammerstein model

The Hammerstein model [5] is represented by a memoryless nonlinearity followed by a filter, see Figure 3.5. The first introduces the nonlinear effect that causes the AM/AM and AM/PM conversions while the filter introduces memory to the system.

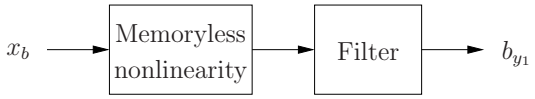

Figure 3.5: Hammerstein model for a nonlinearity with memory.

One of the major problems of using such model is to determine both the nonlinear and linear parts so that the overall response resembles that of the power amplifier to be modeled. Three approaches for the identification of Hammerstein models can be distinguished: iterative approximations [77], correlation techniques [15] and techniques based on least squares estimation and singular value decomposition [10].

The Wiener model

In the Wiener model [87] the nonlinearity is placed after to the filtering effect as it is shown in Figure 3.6. As in the Hammerstein model there are different approaches to determine the response of both the nonlinear and linear parts of the model. The reader is referred to [49, 102, 103] and the references therein.

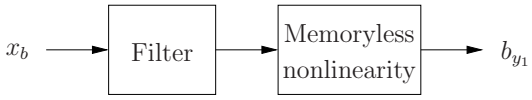

Figure 3.6: Wiener model for a nonlinearity with memory.

Filter-Nonlinearity-Filter model

Both Hammerstein and Wiener models are special cases of a more general model that consists of two filters and a nonlinearity as shown in Figure 3.7. The additional filter introduces another degree of freedom which should produce a better fit for the frequency-dependent AM/AM and AM/PM curves [57].

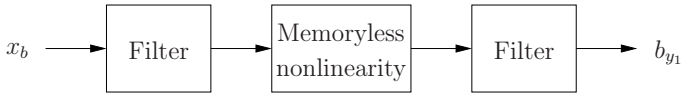

Figure 3.7: Filter-Nonlinearity-Filter model for a nonlinearity with memory.

3.3 Operating point of the amplifier

From Figures 3.2, 3.3 and 3.4 one can see that setting the operating point of the amplifier close to saturation leads to a highly-nonlinear amplification. On the other hand, if the operating point is set far from saturation then the amplifier becomes more and more linear.

The operating point of an amplifier is commonly defined by the input back-off (IBO) and the output back-off (OBO) parameters. IBO is defined as the ratio between the input saturation power of the amplifier and the average power of the input signal

$$\text{IBO} = 10\log_{10}\left(\frac{P_{\text{max,in}}}{\sigma_x^2}\right) \text{ [dB]}. \tag{3.30}$$

Parallelly, OBO is defined as the ratio between the output saturation power of the amplifier and the average power of the output signal,

$$\text{OBO} = 10\log_{10}\left(\frac{P_{\text{max,out}}}{\sigma_y^2}\right) \text{ [dB]}. \tag{3.31}$$

Where, the output saturation power of the amplifier is the maximum total power available from the amplifier and the input saturation power is the drive power at which the output saturation power occurs. Figure 3.8 depicts the concept of IBO and OBO.

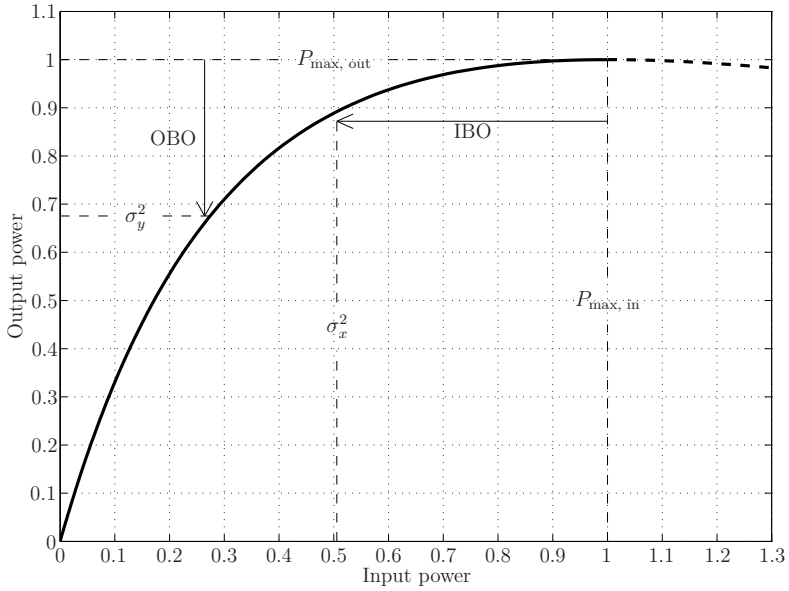

Figure 3.8: Input and output back-off.

As it can be observed, due to the nonlinear amplification of the input signal, the average output power is not equal to the amplification of the average input power, i.e. $\sigma_y^2 \neq G(\sigma_x)^2$. Therefore, the value of OBO for a given IBO will depend on the distribution of the envelope of the input signal. In Figure 3.8 a complex Gaussian distributed signal with appropriate average power (σ_x^2) to assure an IBO=3dB is driven to the input of the nonlinearity.

It is interesting to notice that for Rapp and Ghorbani models an input power equal to infinity is required to achieve the output saturation power, i.e. $P_{\text{max, in}} = \infty$. Therefore, for such models, the concept of IBO as defined in (3.30) becomes meaningless. A possible solution is to define the back-off from 1dB below the saturation point.

Chapter 4

Nonlinearity in MC and MC-SS systems

This chapter analyzes both the statistics of the OFDM-based multicarrier and multicarrier spread-spectrum signals, and the performance of such systems when a nonlinearity is present. The analytical formulation developed in this chapter will be used to define the strategies to be followed with the aim of designing efficient nonlinearity compensation techniques.

4.1 Nonlinearity in multicarrier systems

The block diagram of the system considered in this section is depicted in Figure 4.1. For the sake of simplicity in the mathematical formulation and without any loss of generality the zero padding of the complex baseband modulated symbol vector before the IFFT is done by appending the zeros at the end as shown in (2.13) instead of adding them in the middle of the symbol vector as in (2.15). Moreover, the length of the cyclic prefix is set to zero since no ISI can occur, as an additive white Gaussian noise (AWGN) channel is used.

To analyze the effect of nonlinearities we will first describe the statistics of the input signal $s(t)$ and then we will focus on the output signal $s_d(t)$. Finally, we will see how does it affect the decision variables at the receiver side.

Statistics of the OFDM signal

From (2.9), we recall that an OFDM signal is a sum of many orthogonal subcarriers whose amplitude is determined by the baseband modulated symbols. In general, the baseband symbols can be represented by independent and identically distributed random variables. According to the central limit theorem, if the number of subcarriers

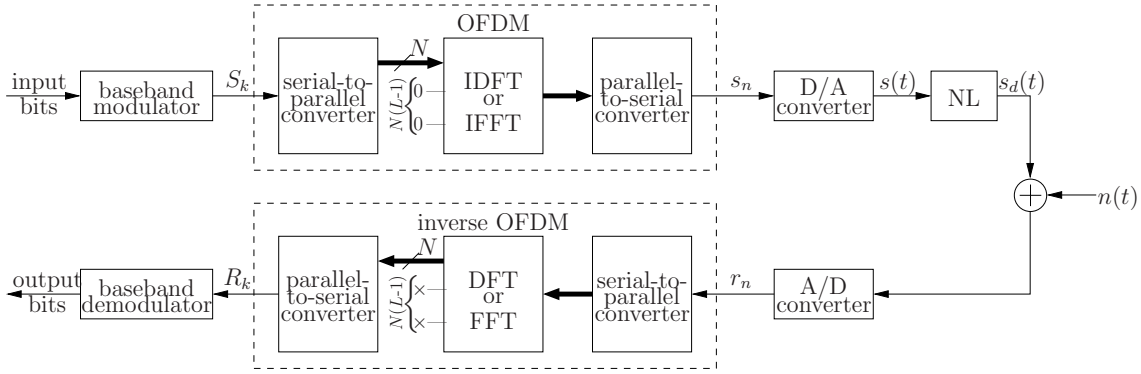

Figure 4.1: Block diagram of an OFDM system with a nonlinearity.

is large enough, the signal can be approximated as a complex Gaussian distributed process. As a result, its envelope follows a Rayleigh distribution as

$$f_X(x) = \frac{2x}{\sigma^2} e^{-\frac{x^2}{\sigma^2}}, \tag{4.1}$$

with

$$E[X] = \sigma \frac{\sqrt{\pi}}{2}, \tag{4.2}$$

$$\text{var}[X] = \sigma^2 (1 - \frac{\pi}{4}), \tag{4.3}$$

where the variance of the real and imaginary parts of the signal is assumed to be $\sigma^2/2$. From a system designer point of view the fact that the envelope of an OFDM signal is Rayleigh distributed essentially means that it suffers from significant fluctuations, thus, a lot of distortion will be introduced when the signal is fed to a nonlinear power amplifier. Being able to quantify the envelope fluctuations of an OFDM signal is twofold. First to determine the HPA power de-rating, i.e. the amount of power back-off needed in the HPA to meet a given adjacent channel leakage ratio (ACLR) level. Second, to design effective techniques to reduce the envelope fluctuations so that the performance of multicarrier systems increases.

Two metrics are mainly used to quantify the envelope fluctuations: peak-to-average power ratio (PAPR) and cubic metric (CM). PAPR is the most common measure of the envelope fluctuations of an OFDM signal. Let $\mathbf{s}^{(m)} = [s_0^{(m)}, s_1^{(m)}, \dots s_{LN-1}^{(m)}]$ be the m-th OFDM symbol generated by (2.10). PAPR of $\mathbf{s}^{(m)}$ is defined as the ratio between its peak power and the average power of all OFDM symbols

$$\text{PAPR}\left(\mathbf{s}^{(m)}\right) = \frac{\|\mathbf{s}^{(m)}\|_\infty^2}{E[\|\mathbf{s}^{(m)}\|^2]/LN}, \tag{4.4}$$

where $\|\cdot\|$ and $\|\cdot\|_\infty$ denote Euclidean and infinity norms, respectively, and the expectation is taken over all OFDM symbols. To evaluate the PAPR characteristics of the

OFDM signal it is customary to compute the probability that the PAPR of an OFDM symbol exceeds a given threshold, in other words one computes the complementary cumulative density function (CCDF) of PAPR.

CM is defined by the Third Generation Partnership Project (3GPP) as [2]

$$\mathrm{CM}|_{\mathrm{dB}} = (\mathrm{RCM}|_{\mathrm{dB}} - \mathrm{RCM}_{\mathrm{ref}}|_{\mathrm{dB}})/K, \tag{4.5}$$

where RCM is called the raw CM, which for a signal $s(t)$, is defined as

$$\mathrm{RCM}\left(s(t)\right)\Big|_{\mathrm{dB}} = 20\log\left[\mathrm{rms}\left[\left(\frac{|s(t)|}{\mathrm{rms}[s(t)]}\right)^3\right]\right]. \tag{4.6}$$

$\mathrm{RCM}_{\mathrm{ref}}|_{\mathrm{dB}}$ is the RCM of the reference signal and K is an empirical slope factor that is used to complete the estimate of the power de-rating required to meet a given ACLR. CM/RCM are often computed over a large signal period corresponding to a large number of OFDM symbols such that a single value for each OFDM system is obtained [28]. In this thesis, the RCM of each OFDM symbol is also independently consider as

$$\mathrm{RCM}\left(\mathbf{s}^{(m)}\right) = \sqrt{E\left[\left(\frac{|\mathbf{s}^{(m)}|^2}{P_s}\right)^3\right]}, \tag{4.7}$$

so that one can obtain the CM characteristics of the OFDM signal by means of the CCDF. In (4.7), $P_s = \sigma^2$ is the average power of the OFDM signal, which is assumed to be constant for all OFDM symbols.

Signal at the output of the nonlinearity

To study the effect of a nonlinear amplifier on the performance of OFDM-based multicarrier systems we will focus on the signal at the output of the nonlinearity. Figure 4.2 shows the power spectral density (PSD) of the OFDM signal at the input, $s(t)$, and the output, $s_d(t)$, of the nonlinearity. As it can be observed, the nonlinearity causes a spectral outgrowth that will interfere neighboring communication systems. The spectral outgrowth can be easily explained from the intermodulation product introduced by the nonlinearity. When two signals of different frequency f_1 and f_2 are passed through a nonlinear device, additional signals, denoted as *intermodulation products*, at frequencies $|mf_1 \pm nf_2|$ may be generated. Spectral outgrowth occurs when the intermodulation products lay outside the transmission bandwidth.

The PSD in Figure 4.2 is computed by means of periodogram, as the average of the PSD, computed by FFT, of each OFDM symbol. This assures that the out-of-band radiation is computed just from the distortion introduced by the nonlinearity. In a practical implementation symbols would be transmitted consecutively in time. This causes an spectral outgrowth due to the transitions between OFDM symbols that can

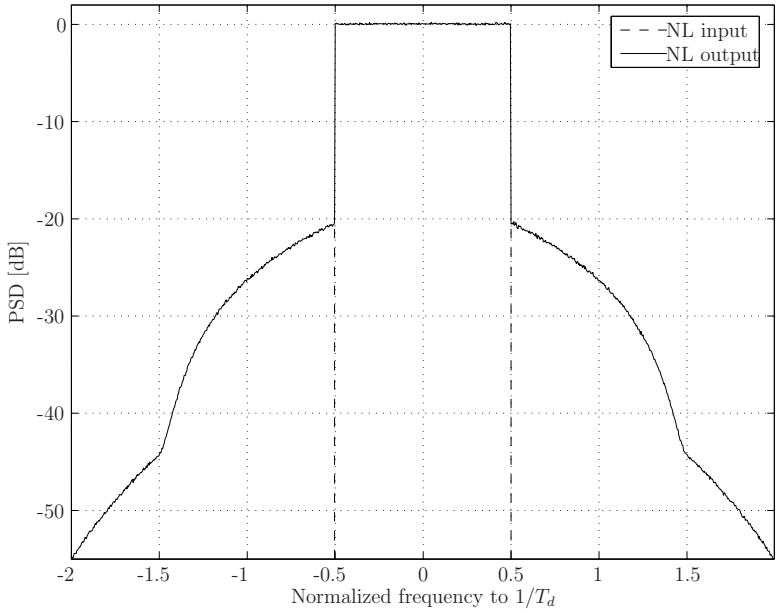

Figure 4.2: Power spectral density at the output of the transmitter.

be reduced by means of windowing.

Let us now analyze the signal constellation after the nonlinearity. As an example we will assume that 16-QAM baseband modulation is used prior to applying OFDM. As it can be seen in Figure 4.3 the signal constellation is largely distorted. In general, the distortion of the constellation can be explained from the in-band intermodulation products. By analyzing the shape of the received constellation two major phenomena can be observed: rotation of the constellation and conversion from a single point to a cloud of points. The first is an effect of the AM/PM characteristic of the nonlinearity, and the second can be explained from the probabilistic distribution of the OFDM signal. It was previously seen that the envelope of an OFDM signal can be approximated by a random variable. Since the envelope of different OFDM symbols is significantly distinct, so will be the effect of the nonlinearity. Therefore, the signal constellation at the output of the nonlinearity will have a probabilistic distribution.

In the remainder of this section a more mathematically rigorous formulation to describe the effect of nonlinearities in OFDM-based multicarrier systems will be presented. This formulation exploits the fact that OFDM signals with large number of subcarriers are complex Gaussian distributed. Let us start by analyzing the Bussgang theorem in [21], which determines cross-correlation functions of two Gaussian signals after one of them has passed through a nonlinear amplitude distortion.

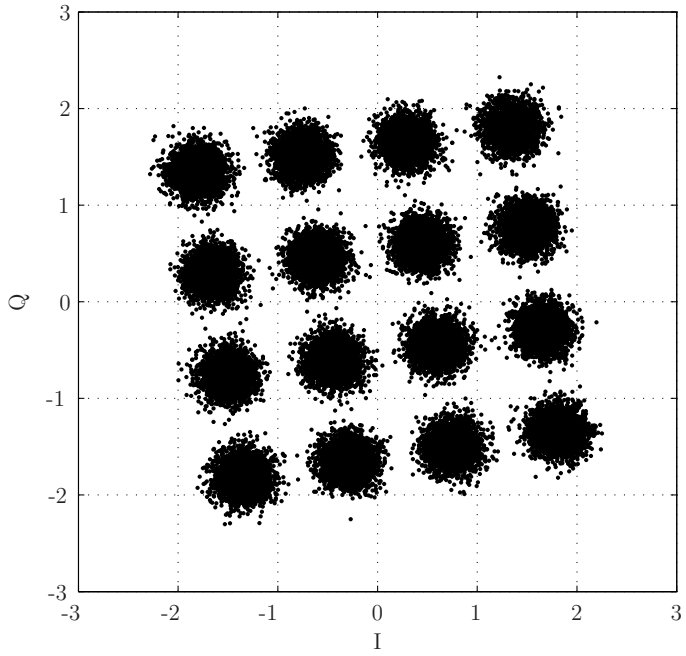

Figure 4.3: Received signal constellation.

THEOREM 1 (BUSSGANG)
For two Gaussian signals $x_1(t)$ and $x_2(t)$, the cross-correlation function taken after one of them (e.g. $x_2(t)$) has undergone nonlinear amplitude distortion ($R_{x_1y_2}$) is identical, except for a factor of proportionality α, to the cross-correlation function taken before the distortion ($R_{x_1x_2}$):

$$R_{x_1y_2}(\tau) = \alpha R_{x_1x_2}(\tau). \tag{4.8}$$

Notice that if $x_1(t) = x_2(t)$ then it follows that the cross-correlation between the input and output signals of the nonlinearity is identical, except for a factor of proportionality α, to the autocorrelation of the input signal, that is

$$R_{xy}(\tau) = \alpha R_{xx}(\tau), \tag{4.9}$$

where, now, the subindices have been removed and, therefore, $x(t)$ and $y(t)$ represent the input and the output signals, respectively.

An interesting result from the Bussgang theorem is that the output $y(t)$ of a memoryless nonlinearity with a Gaussian input $x(t)$ can be written as the sum of a scaled input replica and an uncorrelated distortion term as [29]

$$y(t) = \alpha x(t) + d(t), \qquad \text{where } \alpha = \frac{R_{xy}(\tau_1)}{R_{xx}(\tau_1)}, \tag{4.10}$$

τ_1 is any possible value of τ although usually $\tau_1 = 0$ is chosen. It is easy to show that the distortion term $d(t)$ is uncorrelated with the input signal $x(t)$:

$$\begin{aligned} R_{xd} &= E[x(t)^* \left(y(t+\tau) - \alpha x(t+\tau)\right)] \\ &= R_{xy}(\tau) - \alpha R_{xx}(\tau) \\ &= 0 \end{aligned} \tag{4.11}$$

As it can be observed from the Bussgang theorem, the output signal of a nonlinearity with an OFDM-based input signal is equal to a scaled version of the input signal plus an uncorrelated distortion term. The complex scaling term α introduces a uniform attenuation and rotation to the data bearing tones and, therefore, it is responsible for the attenuation and rotation of the constellation. However, this can be easily compensated at the receiver by introducing a correcting factor $\alpha^*/|\alpha|^2$. On the other hand, the distortion term which is the responsible for both the clouding of the constellation and the out-of-band radiation can not be compensated. Let us define

$$D_k^{(in)} = \begin{cases} D_k \text{ if } k = 0, \ldots, N-1 \\ 0 \quad \text{otherwise} \end{cases} \tag{4.12}$$

and

$$D_k^{(out)} = \begin{cases} D_k \text{ if } k = N, \ldots, LN-1, \\ 0 \quad \text{otherwise} \end{cases} \tag{4.13}$$

then

$$\mathbf{D} = \mathbf{D}^{(in)} + \mathbf{D}^{(out)}, \tag{4.14}$$

where $\mathbf{D} = [D_0, \ldots, D_{LN-1}]$ is the frequency domain representation of the distortion term and $\mathbf{D}^{(in)} = [D_0^{(in)}, \ldots, D_{LN-1}^{(in)}]$ and $\mathbf{D}^{(out)} = [D_0^{(out)}, \ldots, D_{LN-1}^{(out)}]$ represent the in-band and the out-of-band distortion respectively. $\mathbf{D}^{(in)}$ is the part of distortion that increases the bit error rate at the receiver, while $\mathbf{D}^{(out)}$ is, directly, the out-of-band radiation. Note that in order to avoid aliasing the out-of-band distortion into the data bearing tones, sufficient oversampling (normally $L \geq 4$) is required. Figure 4.4 shows the distortion term, computed using Bussgang theorem, of an OFDM system undergoing a nonlinearity. The spectrum is independent of the number of subcarriers and the baseband modulation scheme. As it can be seen $\mathbf{D}^{(out)}$ matches perfectly the shape of the out-of-band radiation and $\mathbf{D}^{(in)}$ introduces an in-band noise.

Signal at the input of the baseband demodulator

Let us now determine the BER performance degradation due to the nonlinearity. The decision variables at the input of the demodulator are

$$R_k = \frac{1}{\sqrt{N}} \sum_{n=0}^{LN-1} r_n e^{-j2\pi kn/LN}, \qquad k = 0, \ldots, N-1. \tag{4.15}$$

By using the Bussgang theorem, the decision variables can be expressed as

$$R_k = \alpha S_k + D_k + W_k \qquad k = 0, \ldots, N-1, \tag{4.16}$$

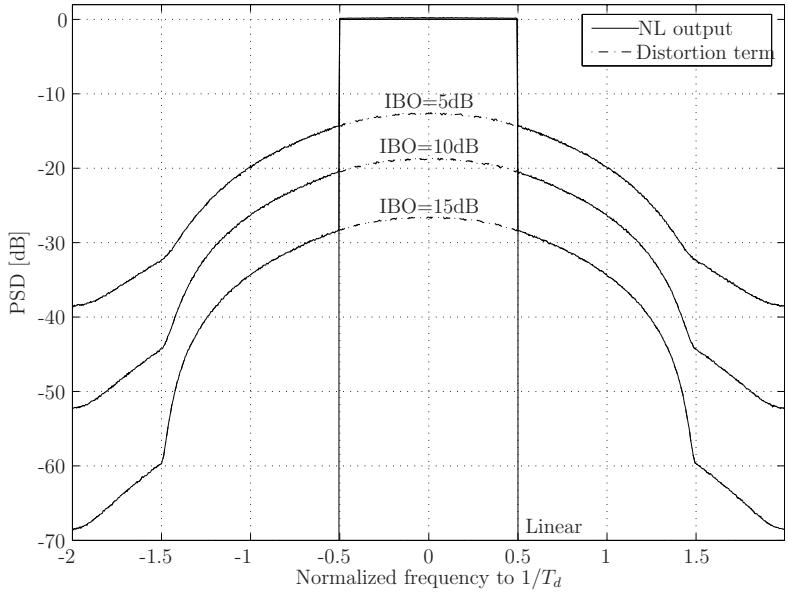

Figure 4.4: Distortion term introduced to an OFDM system by a nonlinearity operating at several IBOs.

where W_k is the Gaussian noise component and D_k is the noise component from the nonlinear distortion.

Let us start by analyzing the Gaussian noise. Let $n(t)$ be a complex white Gaussian noise with variance $\sigma_n^2 = N_0$. At the receiver, after FFT computation, the Gaussian noise at the input of the demodulator becomes

$$W_k = \frac{1}{\sqrt{N}} \sum_{n=0}^{LN-1} n_n e^{-j2\pi kn/LN}, \tag{4.17}$$

which, from the central limit theorem, is also Gaussian distributed. Assuming that $\sigma_n^2 = \sum_{n=0}^{LN-1} |n_n|^2/LN$, $\sigma_W^2 = \sum_{k=0}^{LN-1} |W_k|^2/LN$ and since from the Parseval theorem we know that $\sum_{n=0}^{LN-1} |n_n|^2 = \sum_{k=0}^{LN-1} |W_k|^2$, it can be easily shown that the variance of W_k is $\sigma_W^2 = \sigma_n^2 = N_0$.

Parallelly, the in-band nonlinear distortion noise component can be expressed as

$$D_k = \frac{1}{\sqrt{N}} \sum_{n=0}^{LN-1} d_n e^{-j2\pi kn/LN}, \qquad k = 0, \ldots, N-1. \tag{4.18}$$

which, after noting that it is the sum of N identically distributed random variables, it is reasonable to assume it to be complex Gaussian distributed even though the terms of the sum are not uncorrelated [29]. The nonlinear distortion noise component has zero mean and variance

$$\sigma_D^2 = E[|S_d|^2] - |\alpha|^2 E[|S|^2], \tag{4.19}$$

where S and S_d represent the baseband modulated symbols at the input and the output of the nonlinearity, respectively.

From (4.16), the signal to noise-plus-distortion ratio (SNDR) in AWGN channels can be defined as

$$\text{SNDR} = \frac{|\alpha|^2 E[|S|^2]}{\sigma_W^2 + \sigma_D^2}. \tag{4.20}$$

Notice that due to the Gaussianity of both W_k and D_k, the analytical bit-error probability can be evaluated as a function of the modulation and the total noise that comes from the addition of the AWGN term, W_k, and the nonlinear distortion noise component, D_k. Figure 4.5 shows the simulated and analytical BER performance of an OFDM-based multicarrier system when a nonlinearity is present. The attenuation and rotation of the constellation has been compensated by introducing a correcting factor $\alpha^*/|\alpha|^2$.

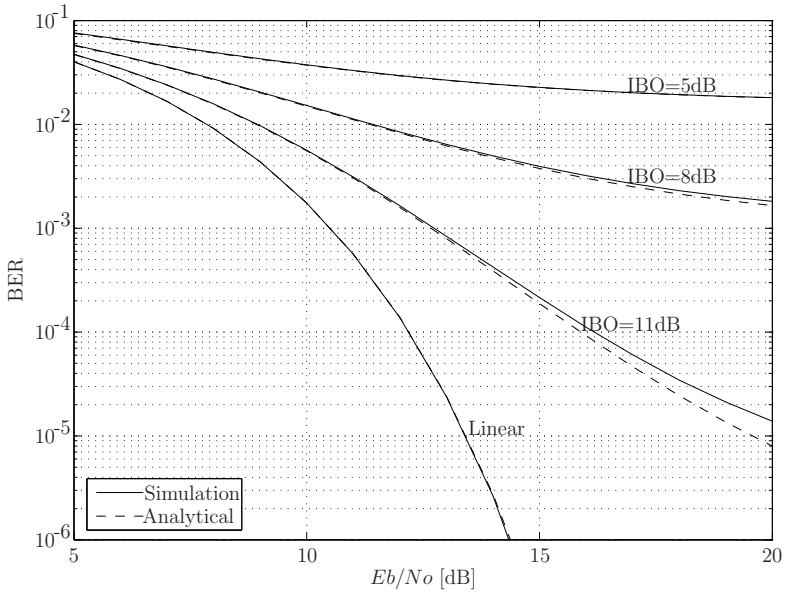

Figure 4.5: Bit-error-rate versus Eb/No at several IBOs for 16-QAM OFDM.

It can be seen that the simulated and analytical results are very close to each other. However, for large IBOs the difference between simulation and analytical results is larger than for low IBOs. Since the amplifier is more linear for large IBOs, less distortion is introduced and therefore the distortion term introduced to the decision variables becomes less Gaussian distributed. The Gaussianity of a random variable can be determined by its kurtosis [53]. Let x be a random variable then the kurtosis of x is defined as [53]

$$\text{kurt}(x) = E[x^4] - 3\left(E[x^2]\right)^2. \tag{4.21}$$

It can be shown that if x follows a Gaussian distribution, its kurtosis $\text{kurt}(x)$ is zero [53]. However, let x be any random variable, then if its kurtosis is negative x is said to be *sub-Gaussian* and if its kurtosis is positive then x is said to be *super-Gaussian*. sub-Gaussian probability density function (PDF) tend to be flatter than the Gaussian one while super-Gaussian PDF has a sharper peak and longer tails than the Gaussian PDF. The normalized kurtosis is defined as

$$\tilde{\kappa}(x) = \text{kurt}(x) / \left(E[x^2]\right)^2 . \tag{4.22}$$

For the real part of the nonlinear distortion D_k, the normalized kurtosis is 0.039, 0.063 and 0.087 for an IBO=5dB, 8dB and 11dB respectively. As it can be observed D_k is less Gaussian distributed for high IBOs and, therefore, the analytical solution that assumes the distortion term to be Gaussian becomes less accurate.

Distortion term introduced by a soft limiter nonlinearity

The non-Gaussian distribution of the distortion term at high back-off becomes more important when a soft limiter (SL) nonlinearity is used. A soft limiter can be seen as a device that is linear below the saturation point and clips all samples exceeding the saturation point to this value. That is, let $x_b = u_x e^{j\alpha_x}$ be the baseband signal at the input of a soft limiter with A being the maximum output amplitude allowed then the baseband output signal becomes

$$y_b = \begin{cases} x_b & \text{if } u_x \leq A \\ Ae^{j\alpha_x} & \text{otherwise} \end{cases} \tag{4.23}$$

From (4.18), the nonlinear distortion noise component is the sum of N identically distributed random variables. Therefore as stated in [29] it is reasonable to assume it to be complex Gaussian distributed even though the terms of the sum are not uncorrelated. However, when a soft limiter nonlinearity that is set to operate at a high back-off is used, $\alpha \simeq 1$, and the distortion term in the time domain is only formed by few delta functions (typically one or two). Therefore, the frequency domain representation of the distortion is equal to the sum of few identically distributed random variables, which is not Gaussian distributed. Figure 4.6 shows the cumulative density function (CDF) of the real part of the in-band distortion introduced by a soft limiter to an OFDM signal. For each IBO the CDF of a zero-mean Gaussian random variable with equal variance to the real part of the in-band distortion is also shown. It can be seen that the in-band distortion follows a complex Gaussian distribution only when the distortion is large enough, i.e. when the soft limiter is set to operate at low back-off.

Let us now analyze the kurtosis of the noise component from the nonlinear distortion introduced by a soft limiter to an OFDM signal. Table 4.1 shows the normalized kurtosis of the real part of D_k. For low back-offs the normalized kurtosis is approximately zero, while for large back-offs the normalized kurtosis is very large. Hence the in-band distortion can only be said to follow a complex Gaussian distribution when the soft limiter is set to operate at low back-offs. When large back-offs are used the in-band distortion tends to follow a complex super-Gaussian distribution.

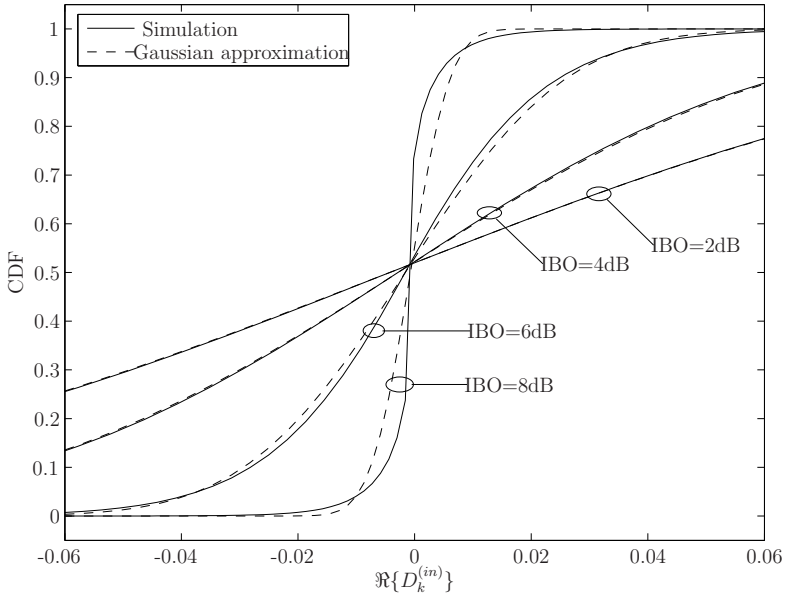

Figure 4.6: Simulation and Gaussian approximation of the CDF of the real part of the in-band distortion introduced by a SL to an OFDM system.

IBO=2dB	IBO=4dB	IBO=6dB	IBO=8dB	IBO=10dB
0.037	0.125	0.976	14.496	386.084

Table 4.1: Normalized Kurtosis of the real part of the in-band distortion introduced by a SL to an OFDM system.

4.2 Nonlinearity in multicarrier spread-spectrum systems

In this section, the effect of nonlinearities in OFDM-based MC-SS systems is evaluated. A MC-SS system is an OFDM system where each data symbol is spread either in time or frequency domain. Therefore, to analyze a MC-SS system, the knowledge that was obtained from the analysis of the effect of nonlinearities in OFDM-based multicarrier systems will be used. Even though the only difference between MC and MC-SS systems is that in the latter the code domain is exploited, this will introduce many different variables to be considered: the type of MC-SS system (MC-CDMA, SS-MC-MA, etc.), the length of the spreading code, the type of spreading code that is being used (Walsh-Hadamard, Golay, DFT-codes, etc.), the number of active codes, etc. For the sake of clarity, and since an extended analysis of multicarrier systems in the presence of nonlinear amplification has not been provided yet, in this section only some basic concepts to understand the effect on nonlinearities in MC-SS systems will be introduced.

The effect of a nonlinearity in a MC-SS system basically depends on the signal envelope and the properties of the spreading codes. Let us start by considering the signal envelope characteristics. In an OFDM system the signal is generally Gaussian distributed and, therefore, nonlinear amplification produces the same effect regardless of the system configuration (number of subcarriers and mapping scheme). The distribution of the MC-SS signal depends on the system configuration, and so does the system performance. As a result, in order to minimize the sensitivity of a MC-SS system to nonlinear amplification one has to properly choose the transmission configuration. A common approach is to use a configuration that reduces the PAPR or CM of the transmitted signal. Recall that in an OFDM system, PAPR and CM can only be used to determine the HPA power de-rating or to design effective techniques to reduce the envelope fluctuations.

Let us now discuss the distribution of the MC-SS signal. The purpose of studying the distribution of the MC-SS signal is to know whether one can use the mathematical formulation introduced in Section 4.1. Roughly speaking, one could say that according to the central limit theorem, in order for a signal to be Gaussian distributed it must be generated by summing many independent and identically distributed random variables. In an OFDM system, the variables that are summed up to generate the OFDM signal are the different subcarriers. One one hand, the subcarrier amplitudes are determined by the baseband modulated symbols which can be approximated as independent and identically distributed random variables. On the other hand, a large number of subcarriers is usually used. Therefore, the Gaussianity assumption in OFDM is valid. However, in a MC-SS this is not always true. In general, it can be said that the Gaussianity assumption will not hold if a few number of subcarriers and few active spreading codes are used. Let us consider the extreme case where just a single bi-valued $\{-1, 1\}$ spreading code is used. In such case the subcarrier amplitudes would at most differ in the sign $\{-d, d\}$, where d represents the baseband modulated symbol, and therefore one could not assume them to be independent random variables. Nevertheless, if a sufficient number of active codes is used, the signal can still be assumed to be Gaussian distributed even though the number of subcarriers is not very large. Note that as the number of active codes increases, the subcarrier amplitudes tend to be more independent.

Let us consider the impact of the system configuration on the OFDM signal envelope. As it will be further discussed in subsequent chapters, one way of reducing the sensitivity of the OFDM signal to nonlinear amplification is by reducing the envelope fluctuations. The type of spreading code, the active spreading codes, etc. play an important role in the envelope of the time domain signal and, as a result, very different performance might be achieved. As an example let us consider three MC-CDMA systems with 16-QAM mapping, namely System-{A,B,C}, each employing a single active spreading code of length $L_{sc} = 16$ and the configuration in Table 4.2. As it can be observed even though the three systems just differ in the active spreading code their

System	Spreading code	Active code	PAPR [dB]	CM [dB]
A	Walsh-Hadamard	1	12.3	23.2
B	Walsh-Hadamard	16	7.5	12.3
C	Golay	1	2.8	4.5

Table 4.2: Configurations of the $L_{sc} = 16$ MC-CDMA systems in Figure 4.7.

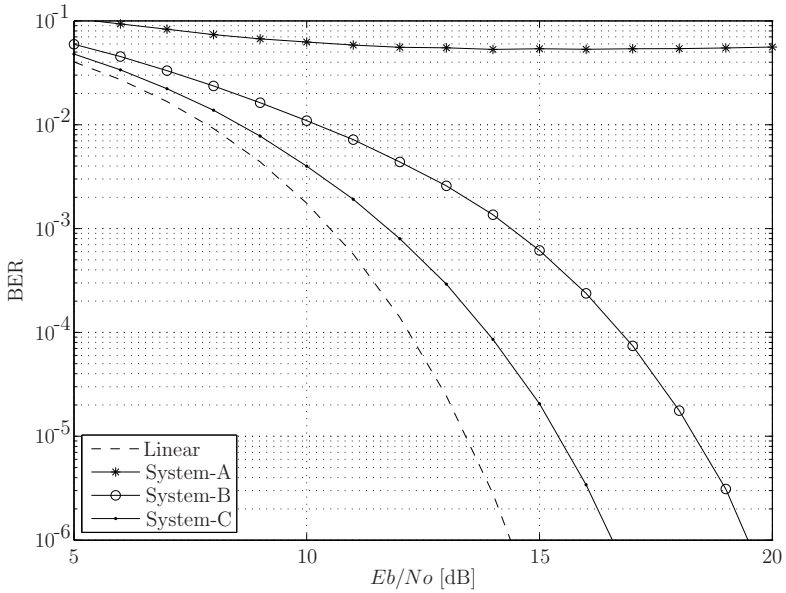

Figure 4.7: Bit-error-rate versus Eb/No for the three $L_{sc} = 16$ MC-CDMA systems with the configurations in Table 4.2. A Saleh nonlinearity operating at 10dB of IBO is used.

average PAPR/CM are very different.

The error probability of the above three systems when a Saleh nonlinearity operating at an IBO of 10dB is used is shown in Figure 4.7. By comparing the average PAPR and CM results in Table 4.2 with the BER performance in Figure 4.7 it can be observed that, as is was already predicted, the larger the envelope fluctuation of the transmitted signal is, the worse the BER performance will be when a nonlinear amplifier is used.

It was previously stated that the effect of a nonlinearity in a MC-SS system basically depends on the signal envelope and the properties of the spreading codes. So far, the dependence on the signal envelope characteristics have only been discussed. Let us now consider the properties of the spreading codes. As it was discussed in Section 2.3 there are several types of spreading codes. In this thesis orthogonal ones are only considered, since they are more likely to be used in practical scenarios. It is widely known that the orthogonality of the spreading codes is lost when the signal is

System	Spreading code	PAPR [dB]	CM [dB]
A	Walsh-Hadamard	6.5	6.9
B	Golay	6.9	7.7

Table 4.3: Configurations and average PAPR/CM of the fully loaded $L_{sc} = 32$ MC-CDMA systems in Figure 4.8.

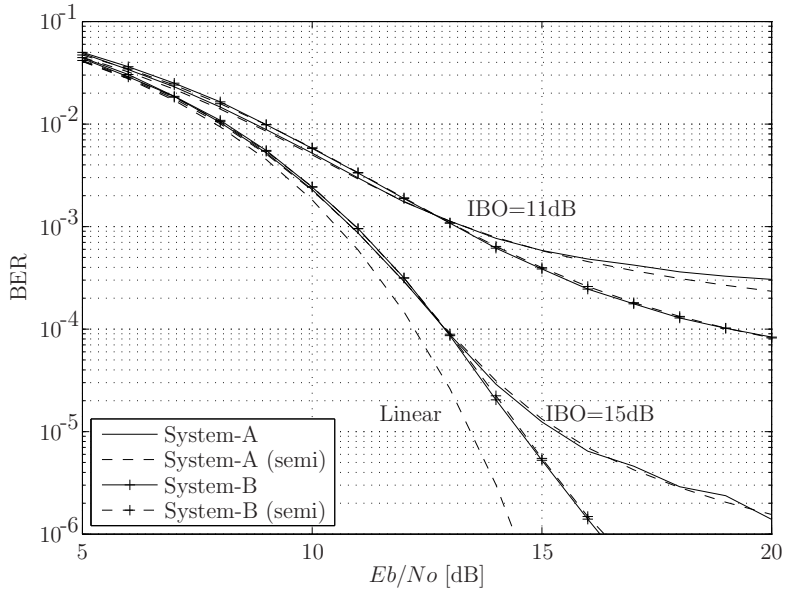

Figure 4.8: Bit-error-rate versus Eb/No for the two fully loaded $L_{sc} = 32$ MC-CDMA systems with the configurations in Table 4.3. A Saleh nonlinearity operating at different IBOs is used.

affected by a multipath fading channel. To reduce the error rate in such cases, using multiuser detection techniques capable of reducing the interference between different spreading codes is necessary. Parallelly, if a MC-SS signal is nonlinearly amplified the orthogonality of the codes is lost and therefore using multiuser detection techniques becomes necessary. Nevertheless, it should be taken into account that the interference generated from one spreading code to another varies according to the active codes and the type of spreading codes. As a result, by choosing the appropriate codes one can reduce interference and therefore the performance improving requirements of the multiuser detector.

From the previous discussion we conclude that in order to reduce the sensitivity of a MC-SS system to the nonlinear amplification one has to choose the spreading codes that minimize both PAPR/CM of the transmitted signal and MAI when orthogonality is lost. A rule of thumb to achieve this, is to list all possible combinations that are known to be more robust to MAI and then choose the one that minimizes the

envelope fluctuations of the transmitted signal. As it will be discussed in subsequent chapters, the combination with minimum envelope fluctuations can be determined by computing the average PAPR/CM of the transmitted signal. On the other hand, the rules to determine the combination of spreading codes that is more robust to MAI can be found in the literature. For instance, see [88] for Walsh-Hadamard codes. In the three systems considered in Table 4.2 and Figure 4.7 there was just one active user and therefore no MAI existed, so choosing the spreading code with minimum PAPR/CM was enough. Let us now consider two fully loaded MC-CDMA systems with 16-QAM mapping, namely System-{A,B}, with $L_{sc} = 32$ Walsh-Hadamard and Golay spreading codes, respectively. At the receiver single user detection is done, so that the MAI introduced by the nonlinearity is not reduced. The average PAPR and CM of each system is shown in Table 4.3 and the error probability is shown in Figure 4.8. As it can be observed, even though the lowest PAPR/CM is achieved by using Walsh-Hadamard codes a better performance is obtained when Golay codes are used. Therefore, both PAPR/CM and the robustness to multiple access interference must be taken into account.

The reader should note that in Figure 4.8 the error rate at different signal to noise ratios is not only computed numerically but also by using semi-analytic simulation. In Section 4.1 it was shown how to compute analytically the error probability of an OFDM system when a nonlinearity is present. However, since such formulation was derived from the Bussgang theorem it can only be used when the Gaussianity assumption holds. A more general way to compute the error probability is by means of semi-analytic simulation. The idea behind semi-analytical simulation is to compute the error probability by using both analytical formulation and numerical computation. In this particular case, the distribution of the constellation at the output of the nonlinearity is first computed by means of simulations. Then, the error probability in AWGN channels is computed analytically by considering that this is actually the constellation that is being transmitted.

Finally we address the difference between uplink and downlink signals since it has an important influence on the Gaussianity of the transmitted signal. In most of the studies of uplink and downlink MC-SS systems from the literature it is assumed that the difference between these two systems is that in the downlink the base station uses all the spreading codes (or at least most of them) while in the uplink each user terminal is assigned just one of them. Therefore, both the user terminal and the base station are assumed to use the same transmission bandwidth and spreading factors. Nevertheless, such configuration is not considered for future OFDM-based wireless communication systems. Instead, OFDMA is used to multiplex different users and spreading is done to transmit the different data symbols within the allocated frequency resources[1]. Therefore in the uplink a fully loaded MC-CDMA system with Walsh-

[1]In fact, this is only true for the uplink since most proposals consider pure OFDMA in the downlink. However, since this section focuses on MC-SS systems, spreading will be assumed in both the forward and reverse links.

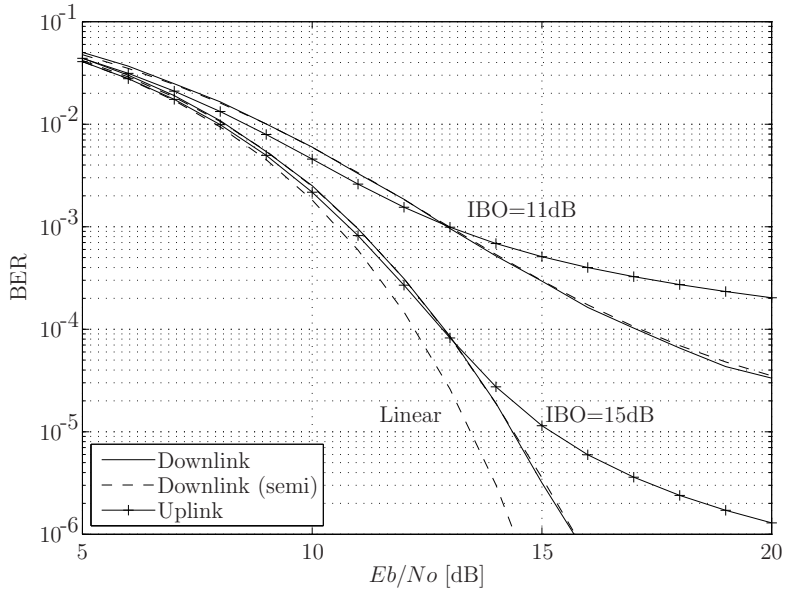

Figure 4.9: Bit-error-rate versus Eb/No for a $L_{sc} = 16$ MC-CDMA system (uplink) and a $L_{sc} = 16$, $N = 512$ SS-MC-MA system (downlink). A Saleh nonlinearity operating at different IBOs is used.

Hadamard spreading codes of length $L_{sc} = 16$ is considered. In the downlink, an $N = 512$ subcarrier, fully loaded SS-MC-MA system also with Walsh-Hadamard spreading codes of length $L_{sc} = 16$ is used. Note that such downlink configuration is equivalent to having 32 fully loaded MC-CDMA users multiplexed in consecutive frequency resources of 16-subcarriers each. Figure 4.9 shows the uplink and downlink performances when a Saleh nonlinearity operating at different IBOs is used. Moreover, the performance of the downlink system is also computed by means of semi-analytical simulations. As it can be observed a better performance is achieved in the downlink, specially for large signal-to-noise ratios.

Chapter 5

Overview of nonlinear distortion compensation techniques

In the previous chapter the effect of nonlinearities in multicarrier systems was analyzed. In this chapter, an overview of the most important nonlinearity compensation techniques for OFDM is presented. Special attention is paid to transmitter side techniques, and more specifically to PAPR/CM-reduction, since they may reduce both the spectral outgrowth and the BER performance degradation when a nonlinearity is present at the output of the transmitter.

It was shown in Chapter 4 that the performance of OFDM-based multicarrier systems is severely affected by the nonlinearity of the high power amplifiers. When an OFDM signal is passed through a nonlinearity both out-of-band radiation and BER increase. As it can be noticed in Figures 4.4 and 4.5, performance degradation of OFDM systems can be reduced by setting the amplifier to operate at high back-offs. However, increasing the back-off means reducing the power efficiency, which is not always an acceptable solution.

There are many strategies to improve the performance of multicarrier systems without having to set the amplifier to operate at large back-offs. One way is to linearize the amplifier response. This is done at the transmitter side and, therefore, it may reduce both the spectral outgrowth and the BER performance degradation. Another solution is to add some processing at the receiver, namely post-processing, that compensates the transmitter nonlinearity such that the BER performance degradation is reduced. Note that, since post-processing is done at the receiver side, it can not reduce the out-of band radiation. The last strategy is to reduce the envelope fluctuations of the transmitted signal. In Section 4.1 we saw that OFDM-based multicarrier signals suffer from large envelope fluctuations. This requires backing-off the power amplifier significantly in order to avoid the signal to be largely non-linearly amplified. By reducing the envelope fluctuations the performance degradation can be reduced, both in terms of BER and spectral outgrowth.

5.1 Linearization

Many linearizing techniques have been proposed to compensate the nonlinear response of the power amplifiers. Those can be categorized into three general types, namely: feedback, feed-forward and predistortion. For a detailed description see [39, 59, 60, 93] and references therein. In general, these techniques require analog circuit design which lies outside of the scope of this thesis. Only predistortion (PD) can be implemented fully digitally. Let us recall from [39] other advantages of predistortion over the other techniques: feedback features conditional stability and is narrow-band and single-carrier oriented. On the other hand, feed-forward is rather expensive and difficult to add to an existing HPA structure. Digital predistortion has in turn proved to be the most suitable solution for adaptive linearization in wideband communications because of its relative simplicity and its ability to be added to existing power amplifiers as separate, low-power consumption, stand-alone units [39, 59].

The idea of digital predistortion is to modify the input signal of the power amplifier so that the output is as close as possible to the linearly amplified original signal. However, since the output power from the amplifier is limited, linearization can only be achieved up to the saturation point.

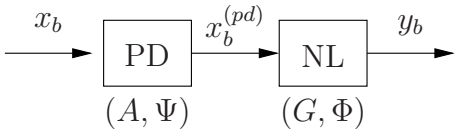

Figure 5.1: Predistortion for NL linearization.

Let us assume a nonlinearity with AM/AM and AM/PM characteristics defined by $G(\cdot)$ and $\Phi(\cdot)$ respectively. Now, assume that the input signal x_b is predistorted by using the AM/AM and AM/PM characteristics determined by $A(\cdot)$ and $\Psi(\cdot)$, respectively, to obtain the signal $x_b^{(pd)}$ that is driven to the nonlinearity. Then, in order to have the output of the nonlinearity y_b equal to the original signal x_b, the AM/AM and AM/PM characteristics of the predistorter must satisfy

$$A(u) = G^{-1}(u), \tag{5.1}$$
$$\Psi(u) = -\Phi(G^{-1}(u)). \tag{5.2}$$

where $G^{-1}(\cdot)$ denotes the inverse function of $G(\cdot)$ such that $G^{-1}(G(u)) = u$, for u smaller that the input saturation level. Let us consider as an example the normalized Saleh model in Figure 3.2, then Figure 5.2 shows the ideal theoretic AM/AM and AM/PM inverse characteristics.

The AM/AM and AM/PM characteristics at the output of the cascade predistorter

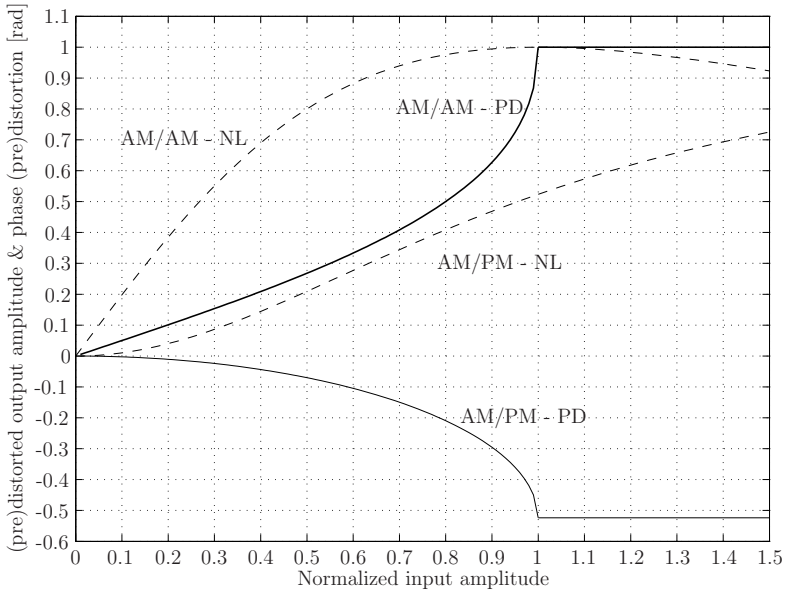

Figure 5.2: AM/AM and AM/PM characteristics of the ideal theoretic predistorter for the Saleh model in Figure 3.2.

and the normalized nonlinearity become

$$G(A(u)) = \begin{cases} u \text{ if } u \leq 1 \\ 1 \text{ otherwise} \end{cases}, \tag{5.3}$$

$$\Psi(u) + \Phi(A(u)) = 0. \tag{5.4}$$

Notice that (5.3) and (5.4) are the AM/AM and AM/PM characteristics of the normalized (i.e. $A = 1$) soft limiter in (4.23). Therefore, the combination of an ideal predistorter plus the nonlinearity becomes a soft limiter. Since, the optimum amplitude-limited nonlinearity that maximizes SNDR is a soft limiter [84], by using predistortion one can maximize the performance of the communication system.

High power amplifiers operating close to the saturation point may undergo slow but significant changes in their AM/AM and AM/PM characteristics, basically due to factors like temperature, power level, frequency changes, age of components and so on. This suggests that predistortion algorithms should be adaptive, thus, able to cope with the time variations of the amplifier response. Different adaptation algorithms have been used to adjust the parameters of a predistorter [23, 92, 105].

5.2 Post-processing

In the previous section, it was shown that by means of predistortion the transmitter nonlinearity can be shaped to become a soft limiter. This assures that the nonlinear

distortion term will have minimum power and, as a result, that the out-of-band radiation is minimized while the SNDR at the receiver is maximized. In this section we will see how to increase the SNDR at the input of the demodulation stage.

The in-band distortion caused by a nonlinearity can be explained from the in-band intermodulation products of the different subcarriers in the OFDM system. Therefore, after the nonlinearity, the k-th subcarrier within an OFDM symbol will be distorted by the other $N-1$ subcarriers in the same OFDM symbol. A solution to reduce the effect of the in-band distortion at the receiver side is to make the decision based on all the data symbols that are transmitted parallelly in each OFDM symbol, i.e. sequence detection. Therefore, the decision on the k-th subcarrier is done based on all received N subcarriers, instead of the conventional symbol by symbol decision. Similar to (4.16), in a multipath fading channel, the decision variables at the input of the demodulation stage can be expressed as

$$R_k = H_k(\alpha S_k + D_k^{(\mathbf{S})}) + W_k \qquad k = 0, \ldots, N-1, \tag{5.5}$$

where H_k is the frequency response of the channel at the subcarrier k and the superscript $(\mathbf{S})$ in $D_k^{(\mathbf{S})}$ is used to stress that the distortion term is a function of the signal vector $\mathbf{S}$. The maximum likelihood (ML) sequence detector must solve

$$\hat{\mathbf{S}} = \arg\min_{\forall \check{\mathbf{S}}} \sum_{k=0}^{N-1} \left| R_k - H_k(\alpha \check{S}_k + D_k^{(\check{\mathbf{S}})}) \right|^2. \tag{5.6}$$

$\check{\mathbf{S}}$ is any possible transmitted signal vector. For an OFDM-based multicarrier system with N subcarriers and baseband modulation constellation of size M, the number of possible transmitted blocks is M^N. Moreover, for each possible transmitted block $\check{\mathbf{S}}$, the corresponding distortion term $\mathbf{D}^{(\check{\mathbf{S}})}$ must be computed. Obviously, solving (5.6) is too complex and, therefore, it becomes necessary to find a suboptimal solution with reduced complexity. Let us start by assuming that the receiver can compute $\mathbf{D}^{(\mathbf{S})}$ [96]. Then, since the distortion term can be eliminated from the decision variables

$$\tilde{R}_k = R_k - H_k D_k^{(\mathbf{S})} \tag{5.7}$$

$$= \alpha H_k S_k + W_k \qquad k = 0, \ldots, N-1, \tag{5.8}$$

the deterministic term $D_k^{(\check{\mathbf{S}})}$ does not play any role in the ML detector. Then (5.6) reduces to

$$\hat{\mathbf{S}} = \arg\min_{\forall \check{\mathbf{S}}} \sum_{k=0}^{N-1} \left| \tilde{R}_k - \alpha H_k \check{S}_k \right|^2 \tag{5.9}$$

$$= \arg\min_{\forall \check{\mathbf{S}}} \sum_{k=0}^{N-1} \left| \alpha H_k \left(\left[\frac{R_k}{\alpha H_k} - \frac{D_k^{(\mathbf{S})}}{\alpha} \right] - \check{S}_k \right) \right|^2. \tag{5.10}$$

The receiver can compute an estimate of $\mathbf{D}^{(\mathbf{S})}$, denoted as $\hat{\mathbf{D}}^{(\mathbf{S})}$, from the received symbol vector $\mathbf{R}$, if it knows the transmit nonlinear function $\mathbf{f}(\cdot)$ and has an initial

estimate of the transmit symbol vector [96]. In the following, a simple iterative quasi-ML algorithm based on hard decoding of the received vector will be described.

1. Compute a hard-decision of the received vector as

$$\hat{\mathbf{S}}^{(q)} = \left[\left\langle \frac{R_0}{\alpha H_0} - \frac{\hat{D}_0^{(\hat{\mathbf{S}}^{(q-1)})}}{\alpha} \right\rangle \cdots \left\langle \frac{R_{N-1}}{\alpha H_{N-1}} - \frac{\hat{D}_{N-1}^{(\hat{\mathbf{S}}^{(q-1)})}}{\alpha} \right\rangle \right]^{\mathsf{T}} = \left\langle \frac{\mathbf{R}}{\alpha \mathbf{H}} - \frac{\hat{\mathbf{D}}^{(\hat{\mathbf{S}}^{(q-1)})}}{\alpha} \right\rangle \tag{5.11}$$

   where q is the iteration number starting with $q = 1$ and $\hat{\mathbf{D}}^{(\hat{\mathbf{S}}^{(0)})} = [\overbrace{00\cdots0}^{N}]$. Note that the first estimation of the transmitted symbol vector is done directly from the received vector, without assuming any knowledge of the distortion term, i.e. $\hat{\mathbf{S}}^{(1)} = \langle \frac{\mathbf{R}}{\alpha \mathbf{H}} \rangle$. The operation $\langle A_k \rangle$ denotes a hard decision, that is, to choose the constellation point that is closest to A_k.

2. Assuming that $\hat{\mathbf{S}}^{(q)}$ is the transmitted symbol vector, compute the corresponding distortion term as

$$\begin{aligned} \hat{\mathbf{D}}^{(\hat{\mathbf{S}}^{(q)})} &= \mathrm{DFT}\left(\hat{\mathbf{d}}^{(\hat{\mathbf{S}}^{(q)})} \right) \\ &= \mathrm{DFT}\left(\mathbf{f}(\hat{\mathbf{s}}^{(q)}) - \alpha \cdot \hat{\mathbf{s}}^{(q)} \right), \end{aligned} \tag{5.12}$$

   where

$$\hat{\mathbf{s}}^{(q)} = \mathrm{IDFT}\left(\hat{\mathbf{S}}^{(q)} \right). \tag{5.13}$$

   and α is obtained as defined in (4.10).

3. Go to step 1 and compute $\hat{\mathbf{S}}^{(q+1)}$ using both the received symbol vector $\mathbf{R}$ and the estimated distortion term $\hat{\mathbf{D}}^{(\hat{\mathbf{S}}^{(q)})}$.

This algorithm was proposed in [96] and similar versions have also been proposed in [12, 24]. Moreover, in [12] soft decision decoding is also considered and shown to offer better performance. A different decision-directed iterative nonlinear decoder was proposed in [61], however this is not ML.

Note that the described algorithm can be split into two parts. First, the impact of the linear multipath fading channel is compensated and then the original signal is computed from its nonlinearly distorted version. In this algorithm the channel response is assumed to be known to the receiver. In a practical implementation, channel estimation is required to obtain the channel response. In an OFDM-based multicarrier system the channel response, which modifies both the amplitude and phase of each subcarrier, is compensated at the receiver side by implementing a bank of one-tap equalizers. To estimate the channel response pilot-symbol-aided channel estimation is done, which is based on multiplexing pilot symbols into the data stream such that they are scattered in both time and frequency directions [72, 91]. Let S_k denote the

transmitted pilot symbol and R_k the corresponding received pilot symbol, the simplest estimate of the channel response can be obtained as

$$\hat{H}_k = \frac{R_k}{S_k}. \tag{5.14}$$

To obtain the channel response at the data bearing tones, two-dimensional interpolation and filtering of the channel response at the pilot tones is done [52]. As in the data bearing tones, the transmitter nonlinearity will introduce a distortion term to the pilot symbols. This will result in an erroneous channel estimation that will degrade the performance of the data recovery process. A better estimate can be obtained by using the pilot symbols at the output of the transmitter nonlinearity, i.e.

$$\hat{H}_k = \frac{R_k}{\alpha S_k + D_k}. \tag{5.15}$$

Since D_k is not known to the receiver, channel estimation and equalization can be incorporated to the iterative quasi-ML algorithm described previously to update the estimated channel response at each iteration [41].

5.3 Reducing the envelope fluctuations

It has been shown that by means of predistortion, SNDR at the receiver can be maximized while the out of-band-distortion is minimized. Moreover, by applying post-processing the effect of the in-band distortion at the receiver side is reduced, thus, increasing the SNDR prior to the demodulation stage. In this section, techniques to reduce the envelope fluctuations of the OFDM signal are discussed. By reducing the envelope fluctuations a further reduction of the nonlinear distortion term can be achieved, thus, decreasing the spectral outgrowth and increasing the received SNDR.

PAPR is the most common measure of the envelope fluctuations of OFDM signals. In fact, most of the techniques in the literature were originally designed to reduce PAPR [50]. This section provides a general description of the techniques that is independent of the signal metric being used. A basic description of the methodologies that are used to implement each technique for PAPR reduction is also provided. Moreover, since it has recently been shown that CM is a more suitable metric than PAPR [1], the implementation of the different techniques for CM-reduction will also be discussed. Even though using CM as a signal metric in MC systems is quite new, some of the techniques have already been reformulated to reduce CM [13, 36, 90].

Clipping

In clipping [70, 78] all the samples exceeding a given threshold are forced to this maximum value. Among all PAPR-reduction techniques clipping is probably the most intuitive one. However, for CM-reduction, it is not easy to see that clipping is still an

interesting technique. When clipping is used for PAPR-reduction both the peak power of each OFDM symbol and the average power are reduced. This motivated many researchers to focus just on the peak-power reduction (i.e. the infinity norm) rather than on the peak-to-average power reduction, specially in complex PAPR-reduction techniques. In a similar way, as shown in [36] reducing CM of an OFDM symbol is equivalent to reducing its 6-th norm. Therefore, in order to reduce CM of a signal one should avoid large magnitudes in the time domain samples. This can be achieved by using a clipping device with a sufficiently low clipping threshold such that a significant number of time domain samples are clipped.

The major disadvantage of clipping technique is that it increases both the out-of-band radiation and BER. Note that clipping a signal can be seen as passing it through a soft limiter nonlinearity. As it was previously shown, when an OFDM signal is passed through a nonlinear device a distortion term that gives rise to both spectral outgrowth and BER, is introduced. Filtering and windowing can be introduced to control the performance degradation, however, they will generate a regrowth in some time-domain samples that will increase both PAPR and CM. In [8,70] repeated clipping and filtering is considered to reduce both PAPR and at the same time decrease the performance degradation. These methods try to compromise between reducing the PAPR of a signal and scarcely increasing their performance degradation. Moreover, they can also be used for CM-reduction.

Tone Reservation

Tone Reservation (TR) technique consists in reducing the envelope fluctuations of a MC signal by reserving a few tones, known as correcting tones, within the transmitted bandwidth and by assigning them the appropriate values. Consider $\mathbf{S}$ as the length-N OFDM symbol vector in the frequency domain with nonzero tones at positions $\mathcal{P}_M = \{p_1, p_2, \ldots, p_M\}$, and $\mathbf{C}$ as the length-N correcting signal in the frequency domain with nonzero tones at positions $\mathcal{Q}_R = \{q_1, q_2, \ldots, q_R\}$, where $\mathcal{P}_M$ and $\mathcal{Q}_R$ are disjoint sets and $R + M = N$. Then, the corrected OFDM symbol in the time domain is computed as

$$\begin{aligned} \bar{s}_n &= s_n + c_n \\ &= \frac{1}{\sqrt{N}} \sum_{k=0}^{N-1} (S_k + C_k) e^{j\frac{2\pi kn}{NL}}, \end{aligned} \tag{5.16}$$

Since $\mathcal{P}_M$ and $\mathcal{Q}_R$ are disjoint sets, it is obvious that the corrected signal is created without introducing any distortion to the data bearing tones. Moreover no transmission of additional information is required. However, this technique suffers from a loss of data rate and an increase in the average energy per bit, which has to be considered in the overall performance of the system.

In PAPR-reduction the correcting tones are referred to as peak-reducing tones and the correcting/corrected signals as peak-reduced/reducing signals. Optimal PAPR-reduction by TR can be obtained by solving a quadratically-constrained quadratic program (QCQP) [94]. However, several low complexity methods have been proposed [34,69,94] that achieve sufficiently accurate suboptimal solutions. In CM-reduction the correcting tones are referred to as CM-reducing tones and the correcting/corrected signals as CM-reduced/reducing signals. Optimal CM-reduction by TR can be obtained by means of an unconstrained convex optimization problem [36]. Nevertheless, a low complexity suboptimal implementation that is shown to find a sufficiently accurate approximation of the optimal solution can be used [36].

In [36] two equivalent suboptimal solutions to reduce PAPR and CM by TR are compared and it is shown that by using CM-reduction not only a larger reduction of the out-of-band radiation is achieved but also the magnitude of the correcting tones is much lower than the required for PAPR-reduction. Moreover, the BER performance improvement capabilities of CM-reduction are larger than those of PAPR-reduction.

Active Constellation Extension

In Active Constellation Extension (ACE), at each OFDM block, some of the outer signal constellation points are extended toward outside of the constellation such that the envelope variations of the resulting block are reduced. The basic idea is to reduce the envelope fluctuations of the transmitted signal without directly increasing the BER by setting some constellation points farther from the decision boundaries than the nominal constellation points. This technique can be applied to any PSK and QAM constellation. However, in general the larger the constellation size is, the lower the number of extensible constellation points will be, resulting in less flexibility and thus less reduction of the envelope fluctuations. Figure 5.3 shows the possible extensions that can be applied to QPSK and 16-QAM. A shadowed area represents that the corresponding constellation point can be extended to any value within this region, while a dashed arrow is used to represent that the constellation point can only be extended in one dimension. If no shadowed area and no dashed arrow overlap a given constellation point it means that no extension is possible. The advantages of ACE are that it is transparent to the receiver, there is no loss of data rate and no side information is required. However, a direct result of the extension of the constellation is the increase in the average energy per bit, that has to be considered in the overall performance of the system.

ACE was first considered for PAPR-reduction [67, 68]. Similar to TR the optimal solution can be obtained by solving a QCQP. However, as stated in [68], obtaining the exact solution of the optimization problem is not only very computationally demanding, but unnecessary as well, if a good suboptimal solution can be reached efficiently. Therefore, the complexity of this technique strongly depends on the complexity of

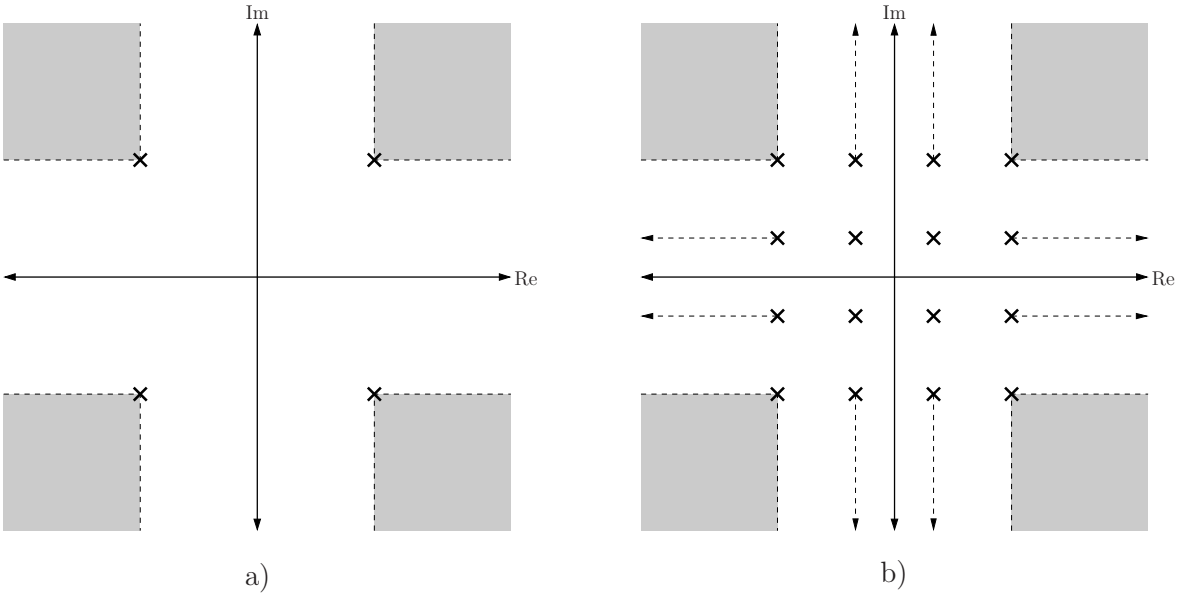

Figure 5.3: Active constellation extension for a) QPSK and b) 16-QAM.

the method used to compute the constellation extension. In [68], a low complexity method to compute ACE is proposed, this method has a complexity requirement of order $\mathcal{O}(N \log N)$, which is basically due to the FFT/IFFT computation.

In CM-reduction, following the method presented in [36] for TR, the optimal solution can be obtained by solving a convex optimization problem. However, since the complexity requirements for computing the optimal solution in ACE are too high for a practical implementation, a suboptimal low-complexity solution is required. Although it has not yet been formally proposed and evaluated it seems that an efficient suboptimal solution can be obtained by using a methodology similar to the one considered in [36], where instead of projecting the CM-reducing signal onto the reserved tones, one would force the ACE constraints.

Tone Injection

Tone Injection (TI) is a technique to reduce the envelope fluctuations similar to ACE. Here, the basic idea is to increase the constellation size so that each of the points in the original basic constellation can be mapped into several equivalent points in the expanded constellation [94]. Since each original symbol can be mapped into several equivalent constellation points, these extra degrees of freedom can be exploited to reduce the envelope fluctuations of each OFDM symbol.

Let $\mathbf{S} = [S_1, S_2, \ldots, S_N]$ be the original symbol vector in the OFDM system, where each data symbol S_k belongs to a square M_k-ary QAM baseband modula-

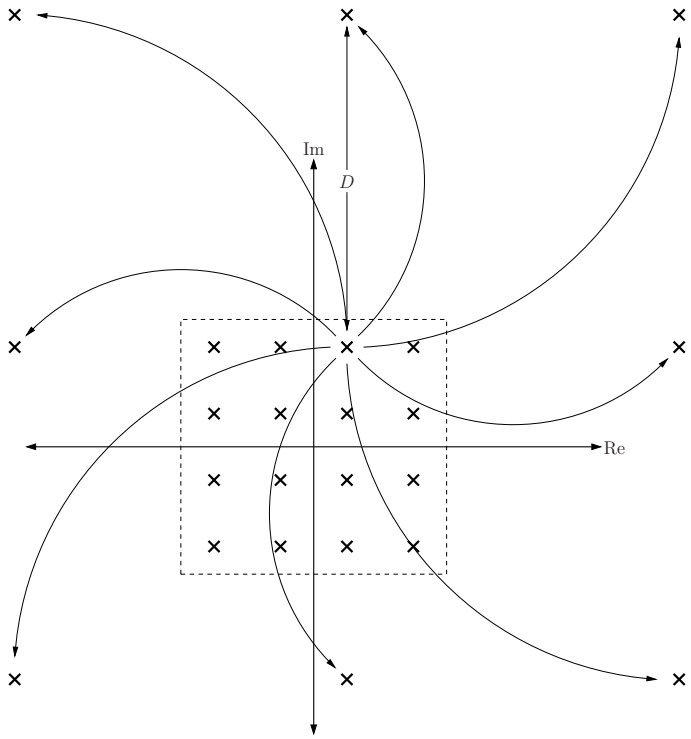

Figure 5.4: Example of tone injection to a 16-QAM constellation point.

tion with a minimum distance d_k between the constellation points. Then, the real and imaginary parts of S_k, denoted as $S_k^{(r)}$ and $S_k^{(i)}$ respectively, can take values $\{\pm d_k/2, \pm 3d_k/2, \ldots, \pm(\sqrt{M_k}-1)d_k/2\}$, where $\sqrt{M_k}$ is the number of levels per dimension. Let us now consider any data symbol S_k, by injecting a tone of the appropriate frequency, f_k, and complex amplitude, $a_k D_k + j b_k D_k$, the original constellation point S_k is mapped to the expanded constellation point $\bar{S}_k = S_k + a_k D_k + j b_k D_k$, where a_k and b_k are any integer values and D_k is a positive real number known at the receiver. According to [94], by choosing $D_k \geq d_k\sqrt{M_k}$, the probability of decoding $\bar{S}_k$ erroneously at the receiver for an uncoded system is roughly the same as the probability of decoding S_k erroneously. To recover the original constellation points at the receiver a simple *modulo-D_k* operation before the baseband demodulation stage is required. This operation requires subtracting/adding multiples of D_k from $\mathrm{Re}\left(\bar{S}_k\right) = S_k^{(r)} + a_k D_k$ and $\mathrm{Im}\left(\bar{S}_k\right) = S_k^{(i)} + b_k D_k$ until they both lie in the interval $[-D_k/2, D_k/2]$.

It is obvious that to minimize PAPR/CM one should determine the appropriate values of a_k and b_k. However, this requires solving an integer programing problem, which has exponential complexity. A simple algorithm to determine the values of a_k and b_k in PAPR-reduction is given in [94]. This algorithm can also be used for CM-reduction. The amount of PAPR/CM-reduction depends on the value of D_k and the number of possible values that a_k and b_k can take. Thus, PAPR/CM-reduction can be

increased by increasing the system complexity. The advantages of TI are that there is no loss of data rate and no side information is required. However, a direct result of the tone injection is an increase in the average energy per bit, which has to be considered in the overall performance of the system.

Selected Mapping

In Selected Mapping (SLM) technique, from the original data block, several candidate data blocks are generated and the one with the lowest envelope variations is transmitted [11,20]. Figure 5.5 shows the block diagram of the SLM technique. First, U different phase sequences of length N are generated, $\mathbf{B}^{(u)} = [b_0^{(u)}, b_1^{(u)}, \ldots, b_{N-1}^{(u)}],\ u = 1, 2, \ldots, U$ where normally $\mathbf{B}^{(1)}$ is set to be an all-one vector of length N in order to include the unmodified data block into the set of candidate data blocks. Then candidate data blocks are generated by element-wise multiplication of the frequency-domain OFDM symbol by each $\mathbf{B}^{(u)}$, IDFT is applied and the resulting block with the lowest envelope fluctuations is selected for transmission. Note that in order to use this technique for PAPR or CM reduction, one only has to use the appropriate criterion in the selection stage, i.e. either minimum PAPR or minimum CM. At the receiver the reverse operation is performed to recover the original data block. Hence, not only the set of U different phase sequences has to be known by the receiver but also information about the selected phase sequence has to be transmitted as side information, which, in fact, is one of the major drawbacks of SLM. It is crucial that this information is received without error, therefore it has to be heavily protected. SLM technique requires transmitting $\lceil \log_2 U \rceil$ bits of side information per OFDM symbol, where $\lceil y \rceil$ denotes the smallest integer that is larger than or equal to y, and has a complexity of U IFFT operations and U complex vector multiplications. The amount of PAPR-reduction depends on the number of candidate data blocks and the design of the phase sequences. Thus, PAPR/CM-reduction can be increased by increasing the system complexity.

Partial Transmit Sequence

In Partial Transmit Sequence (PTS) technique [26, 76, 97], the original data block of length N is partitioned into V disjoint subblocks, $\mathbf{S}_v = [S_{v,0}, S_{v,1}, \ldots, S_{v,N-1}],\ v = 1, 2, \ldots, V$, such that $\sum_{v=1}^{V} \mathbf{S}_v = \mathbf{S}$. The subcarriers in each subblock are phase rotated by the same phase factor, $b_v = e^{j\phi_v},\ v = 1, 2, \ldots, V$, from a set of W possible values. The set of allowed phase factors is written as $P = \{e^{j2\pi l/W},\ l = 0, 1, \ldots, W-1\}$. The phase factors of different subblocks are selected such that the envelope fluctuation of the combined signal is minimized. A block diagram of the PTS technique is depicted in Figure 5.6. At the receiver the reverse operation is performed to recover the original data block. A common method to apply PTS that minimizes the computational complexity without decreasing the capabilities to reduce the envelope fluctuations, is as follows: First, each subblock is independently transformed to the time domain to

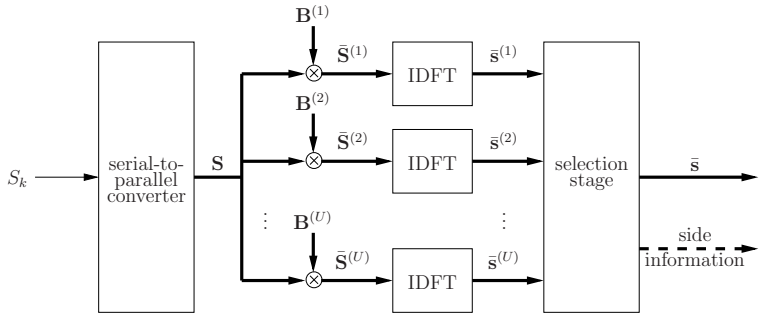

Figure 5.5: Block diagram of the SLM technique.

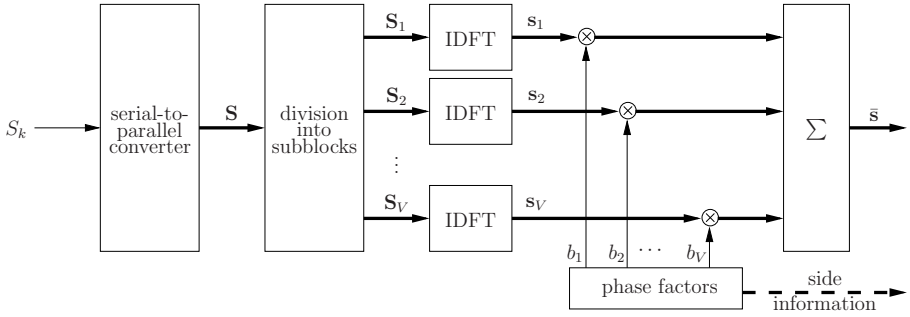

Figure 5.6: Block diagram of the PTS technique.

obtain the so-called partial transmit sequences, $\mathbf{s}_v = \mathrm{IFFT}(\mathbf{S}_v)$. Then, the phase factor of the first partial transmit sequence is set to $b_1 = 1$. This reduces the computational complexity without any loss of performance. To obtain the remaining $(V-1)$ phase factors, exhaustive search among the set P of length W is done. Hence, W^{V-1} combinations of phase factors are evaluated to find the optimum one, i.e. the one that minimizes PAPR/CM. The time domain signal after applying PTS can be expressed as

$$\bar{\mathbf{s}} = \sum_{v=1}^{V} b_v \cdot \mathbf{s}_v, \tag{5.17}$$

where $\{b_1, b_2, \ldots, b_V\}$ is the selected set of phase factors. As in SLM technique, here transmission of side information is required. The number of side information bits per OFDM symbol is $\lceil \log_2 W^{(V-1)} \rceil$. The low complexity implementation of this method requires V IFFTs of the zero-padded length N subblocks, $(V-1)W^{(V-1)}$ complex vector multiplications and $(V-1)W^{(V-1)}$ complex vector sums. In PTS the amount of PAPR/CM-reduction depends on the number of subblocks, V, the number of allowed phase factors, W, and the division of the subcarriers into the different disjoint subblocks. Thus, as in SLM, PAPR/CM-reduction can be improved at the expenses of an increased system complexity.

Interleaving

The interleaving technique is very similar to SLM. Here, several candidate data blocks are generated by interleaving the original data block with different interleavers and the one with lowest envelope variations is selected for transmission [40, 51, 56]. Therefore, as in SLM, this technique can be used for PAPR or CM reduction by using only the appropriate criterion in the selection stage, i.e. either minimum PAPR or minimum CM. An interleaver is a device that operates on a block of N symbols and reorders or permutes them. Let $\mathbf{S} = [S_0, S_1, \ldots, S_{N-1}]$ be the original data block, then the interleaved data block becomes $\bar{\mathbf{S}} = [S_{\pi(0)}, S_{\pi(1)}, \ldots, S_{\pi(N-1)}]$ where $\{k\} \leftrightarrow \{\pi(k)\}$ is a one-to-one mapping with $\pi(k) \in \{0, 1, \ldots, N-1\},\ k = 0, 1, \ldots, N-1$. In order to include the original data block into the set of candidate data blocks the first interleaver is set to $\pi(k) = k,\ k = 0, 1, \ldots, N-1$. To recover the original data block the receiver needs to know which interleaver was used at the transmitter and do the corresponding deinterleaving. Hence, assuming that K candidate data block are generated, $\lceil \log_2(K) \rceil$ information bits have to be transmitted as side information. The amount of PAPR/CM-reduction depends on the number of candidate data blocks, i.e. K, and the design of the interleavers. Thus, PAPR/CM can be reduced by increasing the system complexity. This technique has a complexity of K IFFT operations plus the complexity associated to $(k-1)$ interleavings at the transmitter. At the receiver side only one deinterleaver is necessary.

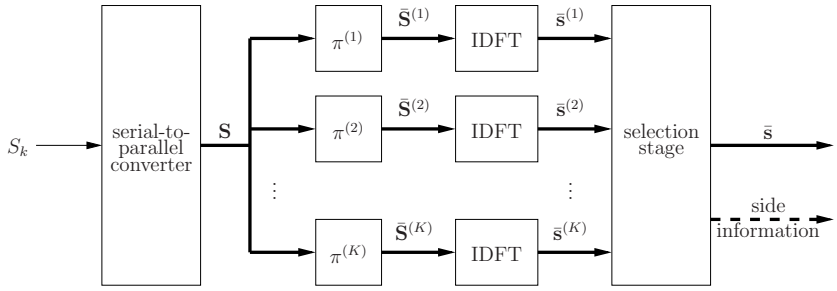

Figure 5.7: Block diagram of the interleaving technique.

Controlled Spectral Outgrowth

In Controlled Spectral Outgrowth (CSO) the envelope fluctuations of each OFDM symbol are reduced by increasing the out-of-band radiation of the nearby subcarriers in a controlled way [37]. Most of the previously described techniques have important drawbacks such as:

- ACE and TI increase the average energy per bit, which degrades the BER performance of the system.
- TR not only increases the average energy per bit but also reduces the spectral

efficiency.

- SLM, PTS and interleaving require the transmission of additional information which increases the energy per bit, reduces the spectral efficiency and increases largely the bit error probability if the side information is received erroneously.

In CSO the envelope fluctuations can be reduced without requiring the transmission of additional information, by a small increase in the average energy per bit and, if some constraints are fulfilled, without reducing the spectral efficiency. Let us define the spectral outgrowth, denoted as η, as the ratio between the extended bandwidth and the bandwidth that occupy the data bearing tones. Then by using a large value of η (typically $\eta \geq 0.5$) the envelope fluctuations can be reduced significantly by a small increase in the transmission power (i.e. the average energy per bit) and without requiring the transmission of additional information. Moreover, this technique is transparent to the receiver. However, in order to avoid reducing the spectral efficiency dramatically, the power spectral density of the out-of-band subcarriers must fit in the spectral mask defined by the different standards. CSO for PAPR-reduction was formulated and evaluated in [37]. For CM-reduction, CSO can be implemented by using methods similar to the one considered in [36].

Coding

A technique specifically designed for PAPR-reduction that was introduced in [58] and developed in [104], is to use block coding to transmit across the carriers only those sequences with small PAPR. This idea is exploited in [30,31] by taking advantage from the relation between Golay sequences and Reed-Muller codes and their properties. Golay sequences [46] are generated as follows. Consider two sequences

$$\mathbf{a} = [a_0, a_1, \ldots, a_{n-1}], \tag{5.18}$$

$$\mathbf{b} = [b_0, b_1, \ldots, b_{n-1}], \tag{5.19}$$

where $a_i, b_i \in \mathbb{Z}_H$ and $\mathbb{Z}_H$ is an integer ring of size H. Then, if the aperiodic autocorrelation of $\mathbf{a}$ and $\mathbf{b}$ at displacement u, defined as

$$C_a(u) = \sum_{i=0}^{n-1} e^{j2\pi(a_i - a_{i+u})/H}, \tag{5.20}$$

satisfies that

$$C_a(u) + C_b(u) = 0, \text{ for each } u \neq 0, \tag{5.21}$$

the sequences $\mathbf{a}$ and $\mathbf{b}$ are called a Golay complementary pair over $\mathbb{Z}_H$ of length n [30,31]. Any sequence which is a member of a Golay complementary pair is called a Golay sequence. The advantage of using Golay sequences in an OFDM-based multicarrier system is that they are demonstrated to have a maximum PAPR of 3dB [81]. On the other hand, Reed-Muller codes are claimed to have good error correction properties

and be easy to decode [75]. In [31] it is demonstrated that each of the $m!/2$ cosets of $\mathcal{RM}(1,m)$ in $\mathcal{RM}(2,m)$ having a coset representative of the form $\sum_{k=1}^{m-1} x_{\pi(k)}x_{\pi(k+1)}$ comprises 2^{m+1} binary Golay sequences of length 2^m, where π is a permutation of the symbols $\{1,2,\ldots,m\}$. Hence, a coding scheme that exploits the relation between Golay sequences and Reed-Muller codes, guarantees a low PAPR while providing a good error correction capability.

The major disadvantage of such a technique is that for practical number of subcarriers (larger than 32) the code rate is too low.